Economic Geology
Vol. 98, 2003, pp. 269–286

Geophysical and Isotopic Constraints on Crustal Structure Related to Mineral Trends in North-Central Nevada and Implications for Tectonic History

V. J. S. Grauch,† Brian D. Rodriguez,

U.S. Geological Survey, Mail Stop 964, Denver Federal Center, Denver, Colorado 80225

and Joseph L. Wooden

U.S. Geological Survey, Mail Stop 937, 345 Middlefield Road, Menlo Park, California 94025

Abstract

We combined information from Sr and Pb isotope data and magnetotelluric models to develop a new magnetic and gravity interpretation of the crustal structure of north-central Nevada to better understand the origin of mineral trends. The new interpretation suggests a crustal structure that is composed of Precambrian continental crust, transitional crust, and primarily oceanic crust that are separated by northwest- and northeast-striking fault zones. The magnetic expression of the buried Precambrian continental crust is recognized for the first time. Low magnetic values primarily reflect magnetite-poor crystalline crust rather than elevated temperatures at depth.

Northwest- and northeast-striking crustal boundaries are defined by isotopic data and abrupt gradients in gravity and magnetic data. The Carlin and Battle Mountain-Eureka mineral trends are associated with two of three northwest-striking boundaries. The Carlin boundary is primarily defined by a change in density and isotopic character of the lower to middle crust. The Battle Mountain-Eureka boundary coincides with a density contrast in the upper crust and a change in isotopic character in the lower to middle crust. Magnetotelluric models suggest that the Battle Mountain-Eureka boundary represents a crustal fault zone for most of its extent, but that deep-rooted faulting is more complex near and northwest of Battle Mountain. Crustal fault zones inferred from the magnetotelluric models near the Carlin trend are oblique to it, suggesting that they may not have been controlled by the deep boundary seen in the gravity and isotopic data. The third northwest-trending boundary is related to the western edge of the buried Precambrian continent in west-central Nevada, but lacks an associated mineral trend. A northeast-striking boundary forms the northern limit of Precambrian continental and transitional crust. The boundaries may have originated as rift or transform faults during Precambrian breakup of Rodinia or as faults accommodating lateral movements or accretion during later Paleozoic tectonic events. Comparing the crustal structure to tectonic elements produced by successively younger events shows that it had a profound influence on subsequent sedimentation, deformation, magmatism, extension, and most important, mineralization.

Introduction

In north-central Nevada, economic geologists commonly have used the alignments of ore deposits with other geologic features, such as igneous bodies, folds, faults, and structural windows, to speculate on the presence of buried regional structures that controlled the alignments (e.g., Roberts, 1966; Shawe, 1991). The two best-known alignments are the northwest-trending Battle Mountain-Eureka (may be called the Cortez gold trend) and Carlin trends (Fig. 1). Evidence of the regional structures related to these alignments has been elusive owing to the complex overprinting, masking, and reactivation of the products of multiple tectonic events that have occurred since Precambrian time. Yet understanding these regional structures, and the underlying crustal structure that controlled them, is important for understanding the tectonic evolution of the mineral trends. We define crustal structure as (1) the configuration of regional-scale (i.e., >100 km^2) blocks of oceanic versus continental lower to middle crust that developed as a result of plate tectonic processes, (2) the associated compositional differences in crystalline basement in the upper crust, and (3) the major lateral discontinuities (crustal fault zones, ramps, or sutures) between and within the blocks.

Interpreting crustal structure in the Basin and Range province from geophysical data has been hampered in the past by the masking effects of low-density basin fill and Tertiary magnetic igneous rocks (Mabey et al., 1978; Blakely and Jachens, 1991), lack of discernable magnetic basement anomalies (Mabey et al., 1978; Blakely, 1988), and by the inability to determine the age of buried structures (e.g., Mabey et al., 1978; Catchings, 1992). The masking effects prevented workers from recognizing any geophysical expression associated with the buried, western edge of the rifted Precambrian continent (Elison et al., 1990), which is commonly inferred from the location of the 0.706 isopleth of initial $^{87}Sr/^{86}Sr$ ratios ($Sr_{initial}$ = 0.706; Kistler and Peterman, 1978; Kistler, 1983). This apparent lack of geophysical expression, combined with seismic-reflection data that showed a relatively flat Moho across the state (Klemperer et al., 1986), led to the conclusion that physical-property differences between blocks of Precambrian crust had been obliterated by later extension and magmatism. Thus, it was commonly thought that geophysical data in the Basin and Range province primarily reflected the products of Cenozoic events (Thompson and Burke, 1974; Eaton et al., 1978; Elison et al., 1990).

In this paper, we seek to overturn this notion by reinterpreting gravity and magnetic data in conjunction with updated interpretations of Pb and Sr isotope ratios (Wooden et

†Corresponding author: e-mail, tien@usgs.gov

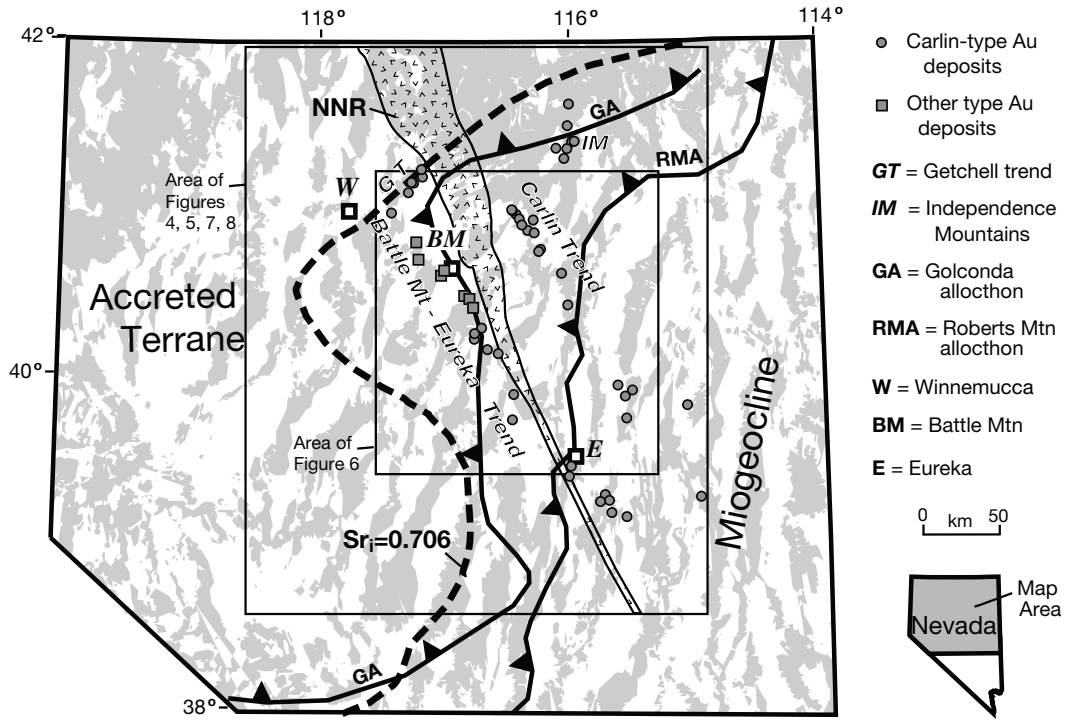

FIG. 1. Major tectonic elements and other features of northern Nevada. Ranges are shaded. RMA and GA mark the eastern limits of the Roberts Mountains and Golconda allochthons, respectively (Stewart, 1980). Northern Nevada rift (NNR) as defined by John et al. (2000) in the north and postulated by Zoback et al. (1994) south of Eureka. The 0.706 isopleth of initial $^{87}Sr/^{86}Sr$ values ($Sr_{initial}$ = 0.706) commonly has been used to mark the edge of the rifted Precambrian continental margin, but more recent analysis indicates that the margin is more complex (Tosdal et al., 2000) (see text). Carlin-type gold deposit locations are from Hofstra and Cline (2000). Labeled are the Battle Mountain-Eureka and Carlin mineral trends and clusters of deposits in the Independence Mountains (IM) and Getchell trend area (GT). Other types of gold deposits (intrusion- and porphyry-related) from McFaul et al. (2000) were chosen to fill in the picture of the Battle Mountain-Eureka trend. Large rectangle shows the area of Figures 4, 5, 7, and 8; small rectangle the area of Figure 6. Cities are Battle Mountain (BM), Eureka (E), and Winnemucca (W).

al., 1998; Tosdal et al., 2000) and of recent results from magnetotelluric geophysical models (Rodriguez and Williams, 2001, 2002). The resulting synthesis for the first time shows a relation between geophysical features in north-central Nevada and the isotopically defined Precambrian rifted margin. It allows for a more comprehensive interpretation of crustal structure that is not possible from one data set alone and improves upon previous gravity and magnetic interpretations that did not establish the tectonic ages of geophysical sources (e.g., Hildenbrand et al., 2000, 2001). Most important, the new interpretation emphasizes the strong spatial relation of mineral trends to the crustal structure inherited from the ancient continent and Precambrian rifting event.

This paper builds on work focused on the Battle Mountain-Eureka trend (Grauch et al., 1995; Grauch et al., 2003). The most recent of these articles documents a crustal fault zone related to the Battle Mountain-Eureka trend using gravity, isotopic data, and magnetotelluric models. In the present paper, we expand our study to cover all of north-central Nevada and add magnetic data to develop a more comprehensive interpretation of the crustal structure. We put the Battle Mountain-Eureka crustal fault zone into context with three other major structures related to the early continental rifting, use the results from the Battle Mountain-Eureka trend to infer the nature of the other structures, and interpret the magnetic data in relation to the isotopic patterns to map the crustal composition between these structures. Another article (Crafford and Grauch, 2002) uses the crustal structure developed in the present paper as a basis for examining the relation of Paleozoic structural domains to mineral trends. In the following sections, we review the isotopic and geophysical data that will be used as constraints, discuss the elements of crustal structure that can be determined from these constraints, build a composite picture of the crust, and finally compare the results to mineral trends and tectonic features of successively younger events.

Tectonic Setting

North-central Nevada has had a complex and varied tectonic history that is part of the evolution of the North American Cordillera. In Late Proterozoic time, the inception of the North American Cordillera during the breakup of the supercontinent Rodinia (e.g., Dalziel, 1997; Karlstrom et al., 1999) was marked by widespread, perhaps intermittent, rifting and ocean-floor spreading (Burchfiel et al., 1992). The breakup led to the development of a west-facing passive margin at the edge of Precambrian continental crust. The location of this edge through north-central Nevada has commonly been inferred from the initial $^{87}Sr/^{86}Sr$ 0.706 isopleth measured from granitoids (e.g., Kistler, 1983; Fig. 1). More recent studies of

Pb and Sr isotope ratios suggest that the rifted margin is more complex and covers a wider area (Wooden et al., 1998; Tosdal et al., 2000). These data are reviewed in more detail in the following section.

Episodes of continental margin modification began with the Late Devonian to Early Mississippian Antler orogeny, where eugeoclinal siliciclastic rocks of the Roberts Mountains allochthon (Fig. 1) were thrust eastward over coeval miogeoclinal rocks of the continental shelf. The orogeny produced an extensive Antler foreland basin (Miller et al., 1992) east of the Roberts Mountains allochthon. A similar event, the Sonoma orogeny, placed eugeoclinal rocks of the Golconda allochthon (Fig. 1) over the Roberts Mountains allochthon and overlapping sedimentary rocks during Late Permian to Early Triassic time (Miller et al., 1992). The Sonoma orogeny culminated in the accretion of oceanic terranes and the establishment of an active continental margin west of Nevada (Burchfiel et al., 1992). Deformation (folding and faulting), crustal thickening, and magmatism related to the active continental margin to the west continued during Mesozoic through early Cenozoic time (Thorman et al., 1991; Burchfiel et al., 1992; Cowan and Bruhn, 1992).

Early to middle Tertiary tectonism was characterized by a southward sweep of generally east-west belts of magmatism from 43 to 21 Ma (Christiansen and Yeats, 1992) and discrete regions of local, highly extended domains (Seedorff, 1991; Wernicke, 1992). Middle to late Tertiary tectonism was characterized by regional uplift, formation of the Northern Nevada rift (Fig. 1), and widespread development of tilted fault blocks and intervening valleys (Basin and Range features) (Christiansen and Yeats, 1992). The mid-Miocene Northern Nevada rift is associated with a prominent, north-northwest–trending linear magnetic high extending for about 500 km, and an alignment of dikes, intrusions, and graben-filling lava flows in north-central Nevada (Zoback et al., 1994; John et al., 2000). This alignment follows a trend east of and slightly divergent from the Battle Mountain-Eureka mineral trend (Fig. 1). Regional uplift and Basin and Range–type extension continues today, accompanied by high heat flow (Sass et al., 1981).

Isotopic Patterns: A Precambrian Legacy

Ascending granitoid magmas commonly retain the geochemical properties of the material near the base of the crust from where they originated. Thus, determining the isotopic compositions of granitoid rocks of different ages gives a general picture of the lower and middle crust through time. Recent studies by Tosdal et al. (2000) and Wooden et al. (1998) show regional variations in isotopic data from primarily Mesozoic- and Tertiary-age granitoid rocks across northern Nevada. These workers examined the spatial distribution of $^{206}Pb/^{204}Pb$, $^{208}Pb/^{204}Pb$, and initial $^{87}Sr/^{86}Sr$ ratios and used the statistical distribution and correlations between the ratios to distinguish three main isotopic provinces (Fig. 2). Wooden et al. (1998) determined slightly different boundaries than shown. The boundary between the western and other provinces, as defined by the 0.706 isopleth of initial $^{87}Sr/^{86}Sr$ ratios ($Sr_{initial} = 0.706$), is commonly inferred as the transition from continental to oceanic crust (e.g., Kistler and Peterman, 1978; Kistler, 1983). The 38.8 and 39 isopleths of $^{208}Pb/^{204}Pb$ ratios (Tosdal et al., 2000; Fig. 2) and the 19.1 isopleth of $^{206}Pb/^{204}Pb$ ratios (Wooden et al., 1998) also broadly define the continental edge. The boundary between the eastern and central provinces, which coincides with the Carlin trend (Fig. 2), was determined primarily by differences in data scatter and correlations between isotopic ratios (Wooden et al., 1998; Tosdal et al., 2000).

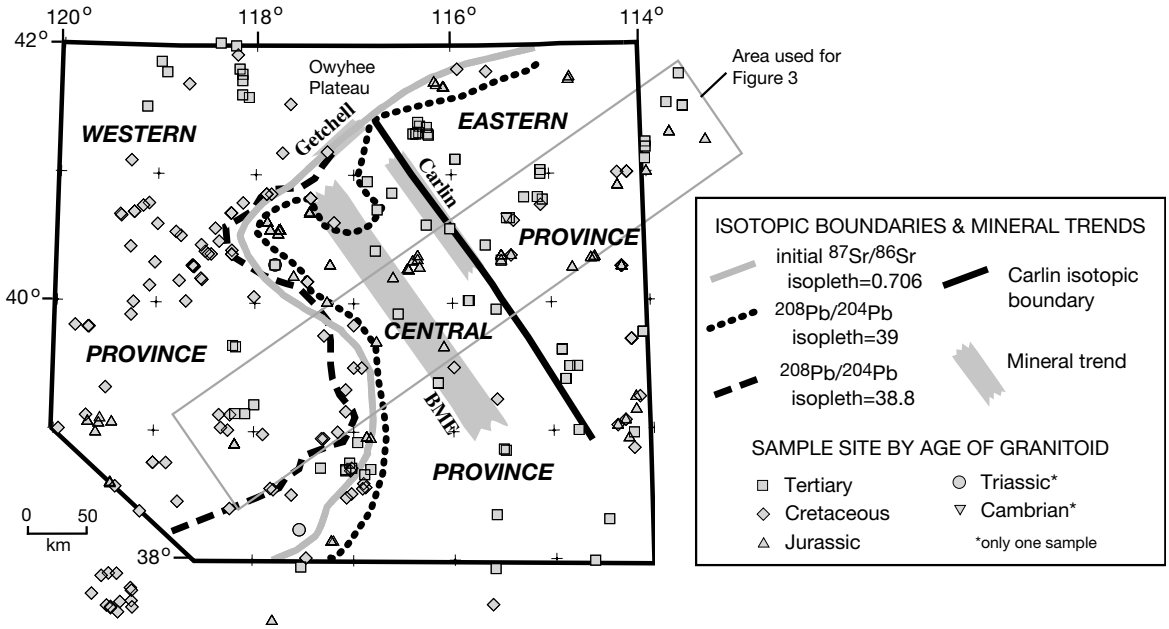

FIG. 2. Isotopic boundaries, provinces, and sample locations for northern Nevada. Isopleths from Pb and initial Sr ratios primarily from Tosdal et al. (2000); Carlin boundary is from Wooden et al. (1998). Sample locations and age of sampled igneous rocks are from Wooden et al. (1999). Ages range from Late Triassic (215 Ma) through middle Miocene (14–15 Ma), with one Early Cambrian (550 Ma) sample. Also shown are the general locations of the Battle Mountain-Eureka and Carlin mineral trends (Fig. 1) and the rectangular box used to select data for the graphs of Figure 3.

The isotope patterns determined from the Pb and Sr data (Fig. 2) are independent of the ages of the sampled rocks (Wooden et al, 1998; Tosdal et al. 2000). This independence implies that the crustal structure reflecting these isotopic patterns had been established by Jurassic time, the age of the oldest samples that show the patterns (Fig. 2). On the other hand, the samples likely are displaced from their original locations because they are mostly older than Mesozoic shortening and Cenozoic extension. However, palinspastic restorations of the $Sr_{initial}$ = 0.706 isopleth show little change in shape; it is translated at most 70 km to the southwest (Levy and Christie-Blick, 1989; Tosdal et al. 2000). This restoration implies that the isotopic province boundaries of Figure 2 generally reflect the crustal boundaries established before Jurassic time.

The western province, generally west and north of the $Sr_{initial}$ = 0.706 isopleth, is composed dominantly of oceanic crust; the eastern province, east of the Carlin trend, represents Precambrian continental crust; and the central province is transitional or thinned crust that formed during development of the passive margin (Tosdal et al., 2000). The crustal compositional differences, the abrupt juxtaposition of crust of different isotopic character, and the shape of the patterns are likely the result of continental margin tectonics (Tosdal et al., 2000). The most significant tectonic event was the Late Proterozic breakup of Rodinia. Other major modifications to the continental margin could have occurred during the Antler and Sonoma orogenies.

The variations in isotopic character that led to the recognition of the province boundaries are evident by plotting the isotopic data from sample sites within a swath perpendicular to the Carlin trend (Fig. 2). Graphs of the data for this swath (Fig. 3), plotted versus distance away from the Carlin trend (eastern-central province boundary), show how the data vary across the province boundaries. The western-central province boundary, which is oblique to the Battle Mountain-Eureka and Carlin trends (Fig. 3), occurs between –150 and –200 km.

The gradual, relatively well grouped, increase of isotopic values from west to east, which is characteristic of the western and central provinces (Wooden et al., 1998; Tosdal et al., 2000), is apparent west of the Battle Mountain-Eureka trend (Fig. 3). Likewise, the highly scattered and wide-ranging isotopic values characteristic of the eastern province are apparent east of the Carlin trend. Between the Battle Mountain-Eureka and Carlin trends, the data appear to increase gradually from west to east but have greater scatter than the data west of the Battle Mountain-Eureka trend (Fig. 3). The mixed isotopic character of the crust between the Battle Mountain-Eureka and Carlin trends indicates that it is intermediate in composition between the crust on either side, and the transition occurs along the Battle Mountain-Eureka trend. Massengill (2001) argued for an even greater contrast in Sr and Pb isotope character along the Battle Mountain-Eureka trend in an independent analysis of another data set. Thus, the isotopic data indicate a contrast in isotopic character of the middle to lower crust at both the Battle Mountain-Eureka and Carlin trends; the contrast is more evident at the Carlin trend than at the Battle Mountain-Eureka trend.

Tosdal et al. (2000) noted the general correspondence of the clusters of deposits of the Getchell trend and in the Independence Mountains to the $Sr_{initial}$ = 0.706 isopleth, which suggests a general association with the buried edge of the Precambrian continental margin. However, they also pointed out that the general orientations of these deposit clusters oppose the strike of the inferred continental margin, indicating a strong local structural control.

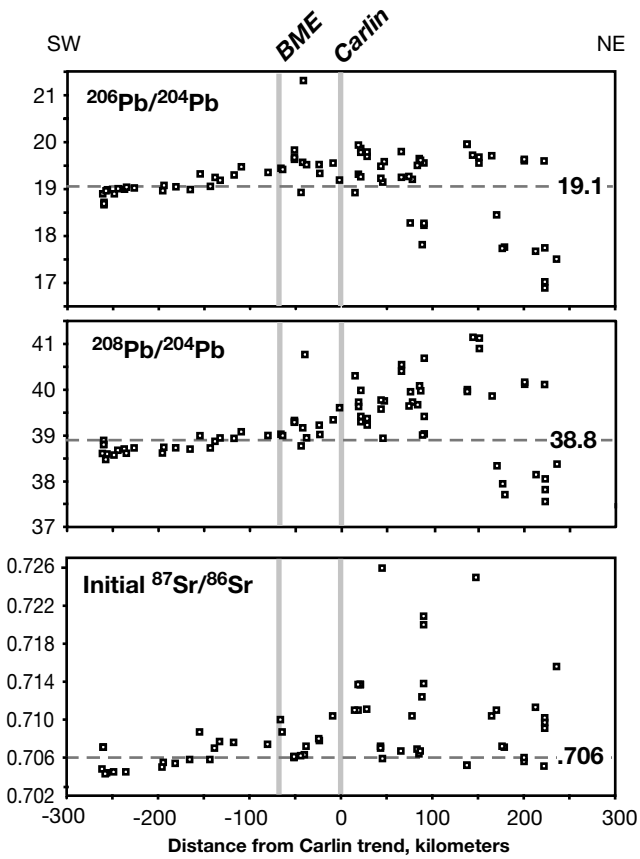

FIG. 3. Graphs of isotopic ratios vs. distance from the Carlin trend (eastern-central province boundary) for data points within the rectangular box shown on Figure 2. Sampled range primarily from Middle Jurassic through Oligocene in age (168–25 Ma). Because of scaling problems, two samples that have initial $^{87}Sr/^{86}Sr$ ratios of 0.737 and 0.738 in the eastern province and one sample with $^{208}Pb/^{204}Pb$ and $^{206}Pb/^{204}Pb$ values of 47 and 25, respectively, located between the Battle Mountain-Eureka and Carlin trends, are not shown. Dashed lines indicate the $Sr_{initial}$ = 0.706 reference and equivalent values for $^{208}Pb/^{204}Pb$ and $^{206}Pb/^{204}Pb$ ratios determined by Wooden et al. (1998). Isotopic character in the area between the Carlin and Battle Mountain-Eureka trends is intermediate between the gradual, well-grouped character to the west of the Battle Mountain-Eureka trend and the wide-ranging, poorly correlated character east of the Carlin trend (see text for discussion).

Gravity Methods: Mapping Density Boundaries

Variations in gravity are caused by lateral variations in rock density. Gravity anomalies occur over volumes of rock having densities that contrast with the surrounding rock. Thus, gravity methods are useful for detecting geologic features that involve the juxtaposition of different rock types, such as faults, anticlines, or folds containing layers of contrasting density.

Gravity field measurements, when processed using standard methods (commonly assuming an average rock density of 2.67 g/cm^3), result in Bouguer gravity data (e.g., Blakely, 1995). However, Bouguer gravity data for Nevada are dominated by the gravity effects of shallow, late Cenozoic Basin

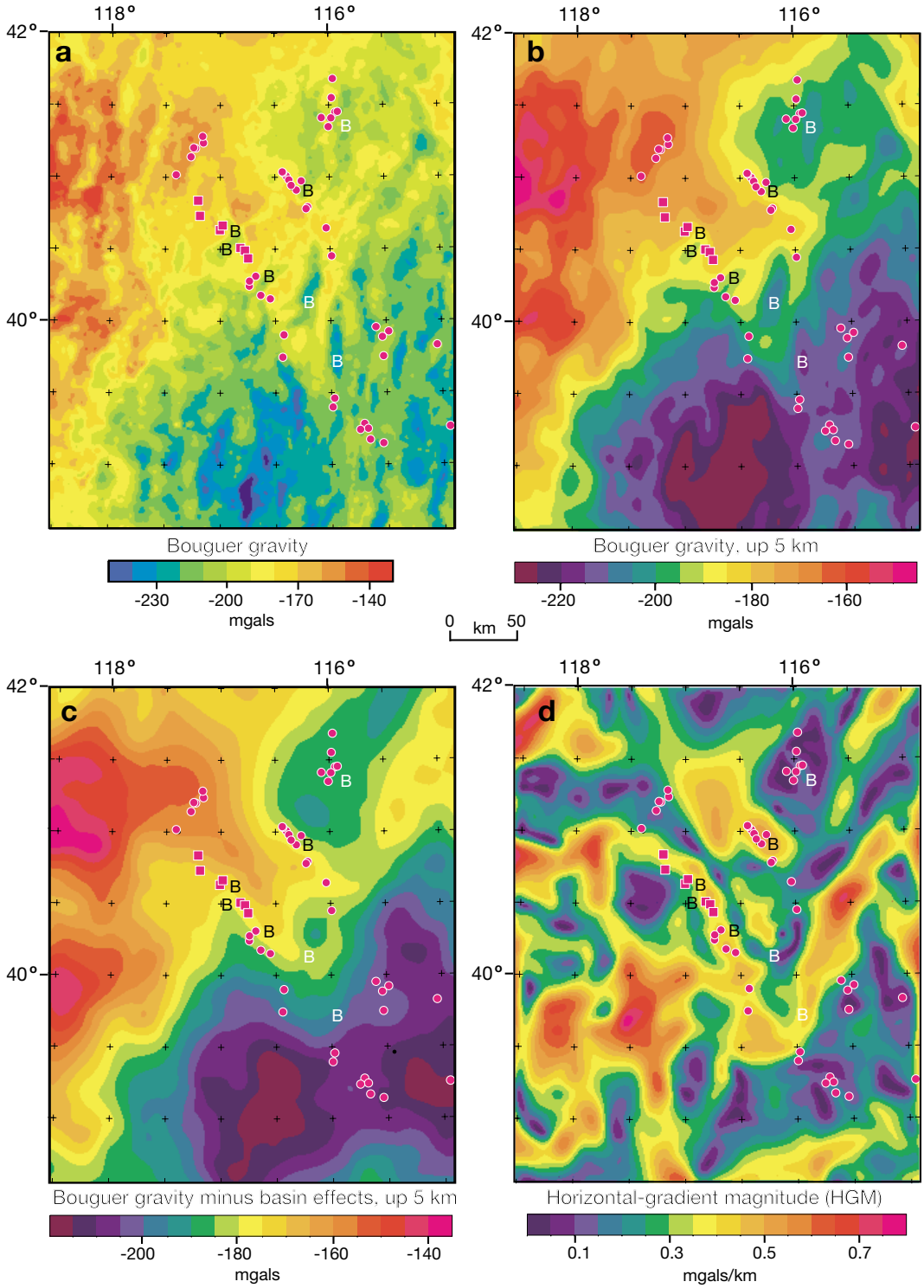

FIG. 4. Bouguer gravity and related maps, showing deposit locations. a. Bouguer gravity data from Ponce (1997). The effects of low-density basin fill (a few are labeled B) masks the broader features. b. Bouguer gravity data analytically continued to an observation level 5 km above ground to enhance broad features and suppress anomalies of limited extent due to shallow sources. Note that some basin effects (B) are still present. c. Bouguer gravity data with effects of gravity models of basins removed (Ponce, 2003) and then continued upward by 5 km. Basin effects (B) are mostly removed and regional gradients associated with both the Battle Mountain-Eureka and Carlin trends are more apparent. d. Map constructed from the gravity data to display ridges where major density boundaries are inferred in the crust. The mapped values are the magnitude of the horizontal gradient of Bouguer gravity of (d) but continued upward by 10 km instead of 5 km to better represent the locations of regional gradients of (c). High horizontal-gradient magnitude values imply either shallow boundaries, boundaries with large density contrast, or both. Density boundaries can represent major fault zones, lithologic contacts (such as the edges of batholiths), or structural relief on the lower crust or mantle.

and Range features, which are evident by numerous elongated, north-south anomalies that mimic topography (Fig. 4a). These effects are suppressed somewhat by upward continuation of the data to a level 5 km higher than originally observed (Fig. 4b). The upward continuation filter enhances broad anomalies and suppresses local anomalies produced by sources of limited depth extent. Removing the gravity effects of geophysical models of the basins prior to upward continuation is more effective at reducing the Basin and Range effects (Fig. 4c). The modeled gravity effects are from Ponce (2003), who followed the iterative gravity modeling method of Jachens and Moring (1990). Regional gradients associated with the Battle Mountain-Eureka trend and the main part of the Carlin trend are more apparent in this map. The trends follow the sides of a southeast-projecting high in the gravity data that generally corresponds to the area of high-density crust found by Hildenbrand et al. (2000). The gradient associated with the Battle Mountain-Eureka trend is more prominent after additional removal of a regional field related to the isostatic compensation of topography, as first shown by Grauch et al. (1995).

The horizontal gradient magnitude (HGM) of gravity data is commonly computed to objectively locate density boundaries associated with gravity gradients (Cordell, 1979), rather than arbitrarily tracing contour lines. The HGM method, analogous to taking a first derivative to locate inflection points of a curve, gives high values where gradients (slopes) in the gravity data are steep. Nearly vertical density boundaries are associated with local maxima in the HGM (Cordell, 1979; Blakely and Simpson, 1986). Thus HGM maps show ridges where there are significant density contrasts in the crust, which commonly occur where different types of crust are laterally juxtaposed.

An HGM map for upward-continued Bouguer gravity with basin effects removed is shown in Figure 4d and discussed in more detail in the section on crustal structure. Several caveats must be kept in mind when one views this map. First, the HGM method is computed within a small window across the grid, which forces the results to focus on gradients related to detailed variations in the data, rather than on the larger, more regional gradients. This enhancement of detail required additional upward continuation of the Bouguer gravity with basin effects removed to 10 km before applying the HGM method (Fig. 4d) in order to enhance the regional gradients that can be seen in Figure 4c. Second, density boundaries are poorly defined by HGM ridges in areas where there is interference from neighboring (or overlying) sources (Grauch and Cordell, 1987). The shallowest density boundaries produce high HGM values that overprint the more subtle expression of deeper boundaries with similar density contrast. Discontinuous local ridges also can be superposed on more subtle regional gradients, such as a regional structural zone expressed as en echelon faults near the surface.

Magnetic Methods: Mapping Magnetic Boundaries and Basement Character

Aeromagnetic surveys measure variations in the strength of the Earth's magnetic field that are produced by changes in magnetization of the crust. Magnetization of rocks is determined by the quantity of magnetic minerals (commonly titanomagnetites), their ability to be inductively magnetized, and the strength and direction of remanent magnetization carried by the magnetic minerals. Igneous and crystalline metamorphic rocks commonly have moderate to high total magnetizations, whereas sedimentary rocks can be considered effectively nonmagnetic when one interprets aeromagnetic surveys at regional scales (Nettleton, 1971), as we do in this study.

Aeromagnetic data for the study area (Fig. 5a) are extracted from a statewide compilation of many individual surveys (Hildenbrand and Kucks, 1988). The aeromagnetic map is dominated by the expression of Phanerozoic igneous rocks (Mabey et al., 1978; Blakely and Jachens, 1991). The most prominent feature is the north-northwest alignment of magnetic highs in the center of the area that corresponds to the Northern Nevada rift (Fig. 5a, b). Several workers have discussed the parallel alignment of magnetic highs to the west (Blakely, 1988; McKee and Blakely, 1990; Glen and Ponce, 2002; Ponce and Glen, 2002), from 118° W longitude at the northern state boundary to Winnemucca, then splitting into two extensions south to about 40° N latitude (E and W in Fig. 5b). Although an analogous rift system is not apparent in rocks at the surface, the similarity in geophysical signature of the anomalies parallel to the Northern Nevada rift suggests a similar genesis (Blakely, 1988).

Regional features that might reflect differences in the buried crystalline basement are difficult to see in the aeromagnetic data (Fig. 5a). To enhance the regional features, the magnetic potential was computed from the data (Blakely, 1995). This transformation, originally called the pseudogravity transformation by Baranov (1957), computes a vertical integral of magnetic data, which can be viewed as an averaging technique that enhances the very broad features of the data. The broad features to be enhanced can extend more than 500 km, so the transformation must be applied to a larger data set in order to properly represent the features that span the edges the study area. In this study, the transformation was applied to the western part of a recent compilation of aeromagnetic data for the United States (North American Magnetic Anomaly Group, 2002), which incorporates the compilation of Hildenbrand and Kucks (1988) for Nevada. The results extracted for the study area are shown in Figure 5c.

To enhance regional magnetic boundaries, the HGM was computed from the magnetic potential data after upward continuation by 5 km (Fig. 5d) following the method of Cordell and Grauch (1985). This map objectively locates the steepest parts of the gradients in the magnetic potential, and is analogous to the HGM maps computed for gravity data. The same caveats apply to magnetic boundaries as were discussed for density boundaries. The boundaries will be discussed further in a later section on crustal structure.

The most conspicuous features of the magnetic potential map (Fig. 5c) are the low values (<80 magnetic potential units—mpu) in the eastern half, which gradually increase in value from east to west, and the moderate (80–115 mpu) to high (>115 mpu) values in the northwest and southwest. The eastern part of the low area (generally east of 116° W) is included in the previously recognized "magnetic quiet zone" or "basement quiet zone" of the eastern Great Basin (Zietz et al., 1970; Mabey et al., 1978; Blakely, 1988, and references therein). In this zone, local magnetic features are subdued and basement magnetic anomalies, which should be present

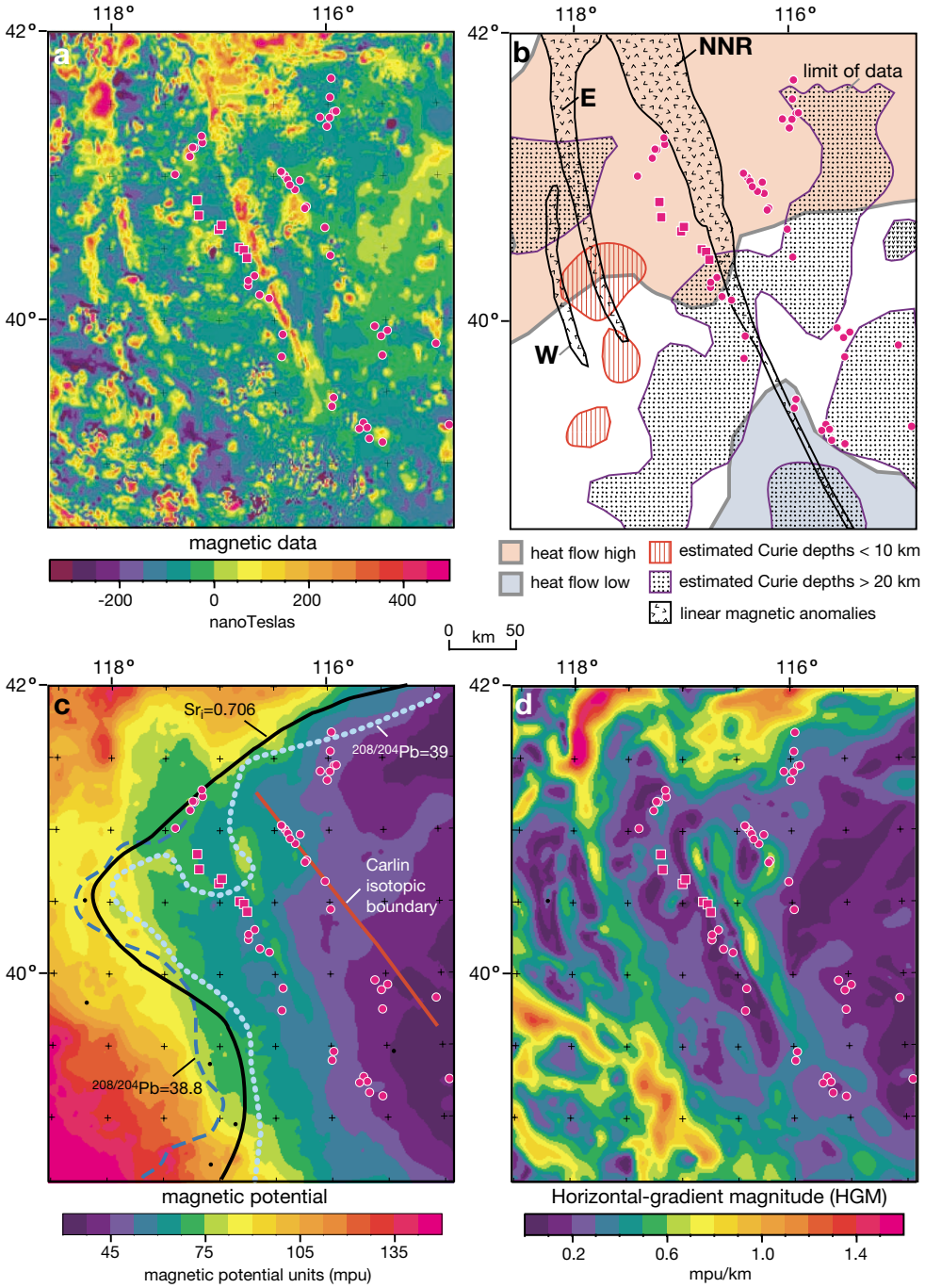

FIG. 5. Aeromagnetic data and related maps, showing deposit locations. a. Aeromagnetic data compiled by Hildenbrand and Kucks (1988) at 300 m above ground. b. Magnetic features compared to heat flow anomalies from (Sass et al., 1981) and Curie depths estimated from aeromagnetic data (Blakely, 1988). The Northern Nevada rift (NNR) is expressed in Figure 5a as the prominent north-northwest–trending alignment of magnetic highs. The Eastern (E) and Western (W) subparallel anomalies look magnetically similar to the Northern Nevada rift but are not related to exposed rocks. Curie depths less than 10 km suggest that basement rocks are not magnetic; those greater than 20 km suggest that basement rocks are magnetic and should produce anomalies. c. Magnetic potential data computed as a vertical integral of the aeromagnetic data that enhances the broadest features of the data corresponding with major crustal features. The units (mpu) are arbitrary. Black, blue, and light blue lines are the isopleths of $Sr_{initial}$ = 0.706 and $^{208}Pb/^{204}Pb$ = 38.8 and 39, respectively, from Figure 2. Lack of correlation between lows on this map and the thermal features of Figure 5b, combined with the good correspondence between the Sr and Pb isopleths and the limits of the region of areas of low values, imply that the low values are primarily produced by magnetite-poor basement rocks rather than elevated temperatures (see text for explanation). d. Map constructed from magnetic potential data to display ridges where major magnetic boundaries are inferred in the crust. The magnetic potential data were continued upward by 5 km before computation of the horizontal-gradient magnitude to highlight regional gradients. The boundaries may represent faulted margins of Precambrian basement, regional contacts between large intrusions and sedimentary country rock, or structural relief on the lower crust.

if the crystalline basement were magnetic, are largely absent (Mabey et al., 1978).

The low magnetic potential values and lack of basement anomalies imply that the bulk of the crust, including the crystalline basement, has low magnetization. The low basement magnetization has been explained by present-day elevated temperatures at depth or by a paucity of magnetic minerals in the rocks (Shuey et al., 1973; Mabey et al., 1978). Elevated temperatures at depth could heat magnetite above 580°C, its Curie temperature. Above this temperature, magnetite loses its magnetization, but it becomes magnetic again once it cools below the Curie temperature. A present-day, shallow Curie depth (the depth to the 580°C isotherm) seems plausible, because elevated temperatures and thin lithosphere are likely in the Basin and Range province. However, there is poor correlation between the area of low magnetic potential and regions of high heat flow (cf. Fig. 5b, c). In addition, shallow Curie depths (<10 km), estimated from the magnetic data, are concentrated on the western and northwestern sides of the study area (Fig. 5b), corresponding more closely with the Battle Mountain heat flow high and the 118° meridian seismic zone (Blakely, 1988) than with the lowest magnetic potential values.

The limits of low magnetic potential show better correspondence with the $Sr_{initial}$ = 0.706 and related Pb isopleths (Fig. 5c). The magnetic-potential limits are generally followed by the light green color band representing values between 75.0 and 82.5 (Fig. 5c) and corresponding ridges in the HGM map (Fig. 5d). The correspondence of the magnetic potential and the isopleths of Sr and Pb ratios is remarkable considering the regional resolution of the isotopic data, the possible tectonic displacement of isotopic samples from their original locations, and the multitude of variations likely present in the magnetic and isotopic properties of the crust. The correspondence implies that the limits of the region of low magnetic values are better explained by the juxtaposition of weakly magnetic Precambrian crystalline basement in the central and eastern provinces against more magnetic basement in the western province than by an abrupt, large difference in crustal temperature. Moreover, the general increase in magnetic potential values from northeast to southwest, allowing for interruption by the expression of the Northern Nevada rift, correlates with the transitions in lower to middle crustal composition inferred from the isotopic data (Fig. 3). We conclude that the low basement magnetization is due to magnetite-poor Precambrian crystalline basement related to continental and transitional crust rather than to elevated temperature. The low magnetic potential values are an expression of these basement rocks, and it follows that the moderate to high magnetic potential values are an expression of the more magnetic crust in the western province. These conclusions are significant because the magnetic expression of the Precambrian crust and its margin have not been recognized previously in north-central Nevada.

The moderate magnetic potential values in the west-central part of the area (Fig. 5c) likely reflect the dominantly oceanic crust of the western province, which is more magnetic than the other two provinces. However, the areas of high magnetic potential values in the northwest and southwest parts of the study area (Fig. 5c) are also areas that were intruded by extensive intermediate to mafic Mesozoic or Cenozoic magmas (Stewart and Carlson, 1977). The dominantly oceanic composition of the crust in the western province combined with the widespread igneous intrusions in the upper crust can account for these regionally high magnetic values. In contrast, areas of widespread igneous intrusions in the central province, such as the Northern Nevada rift, still have fairly low magnetic potential values (Fig. 5c).

A noteworthy exception to the correlation between the area of low magnetic potential and the trace of the isotopic isopleths is northwest of the Getchell trend area (Fig. 1), where moderately low values of magnetic potential continue approximately 50 km northwest of the $Sr_{initial}$ = 0.706 isopleth (Fig. 5c). It is possible that this is a lateral displacement of, or original jog in, the Precambrian crust not resolved in the Sr isotope data. Constraints on the location of the isopleth are poor north and northeast of the Getchell trend area, where late Cenozoic basalt covers the Owyhee Plateau (Fig. 2). This area is discussed further in a following section.

Magnetotelluric Models: Evidence for Crustal Faults

The magnetotelluric method (Vozoff, 1991) measures the natural, time-varying electric and magnetic fields at the surface of the Earth and yields information on the patterns of electrical resistivity (the inverse of conductivity) in the subsurface. Sources of natural magnetic and electric fields are lightning and ionospheric electrical currents found across the globe at a range of frequencies. The range of frequencies produced by the fields allows the operator to adjust the depths of investigation from tens of meters to tens of kilometers through different experiment designs. Laboratory studies have shown that the factors that affect resistivity in the Earth's crust are the composition and temperature of pore fluids, melts, and the presence of clay minerals, graphite, or certain metallic minerals (Keller, 1989). Any of these factors can measurably decrease the resistivity of carbonate and silicate rocks that constitute most of the crust, and thus they allow certain inferences about lithology and structure.

Rodriguez and Williams (2001, 2002) collected magnetotelluric soundings along a series of profiles crossing the Battle Mountain-Eureka and Carlin trends (Fig. 6) and constructed profile models from these soundings assuming a two-dimensional earth. They also distinguished zones of resistivity with two-dimensional structure (elongated oblique to the profile) versus those with three-dimensional structure (spatially limited away from the profile), which were derived by measuring orthogonal components of the electric and magnetic fields at each site. Locating two-dimensional structures is significant because of the widespread three-dimensional character of magnetotelluric data in the Basin and Range province that reflects local complexities (Wannamaker, 1983).

Rodriguez and Williams (2001, 2002) modeled several narrow (about 10 km wide), subvertical, two-dimensional conductors (1–10 ohm-m) that penetrate from 1 to 5 km below the surface to midcrustal (20 km) depths along the profiles. The conductors are best explained as crustal-scale fault or fracture zones (Eberhart-Phillips et al., 1995). The very low resistivities are likely caused by material associated with faulting or fracture filling, such as argillic or clay alteration, mylonitic breccia, graphitic carbon associated with shearing, brine-filled fractures, or a combination of these.

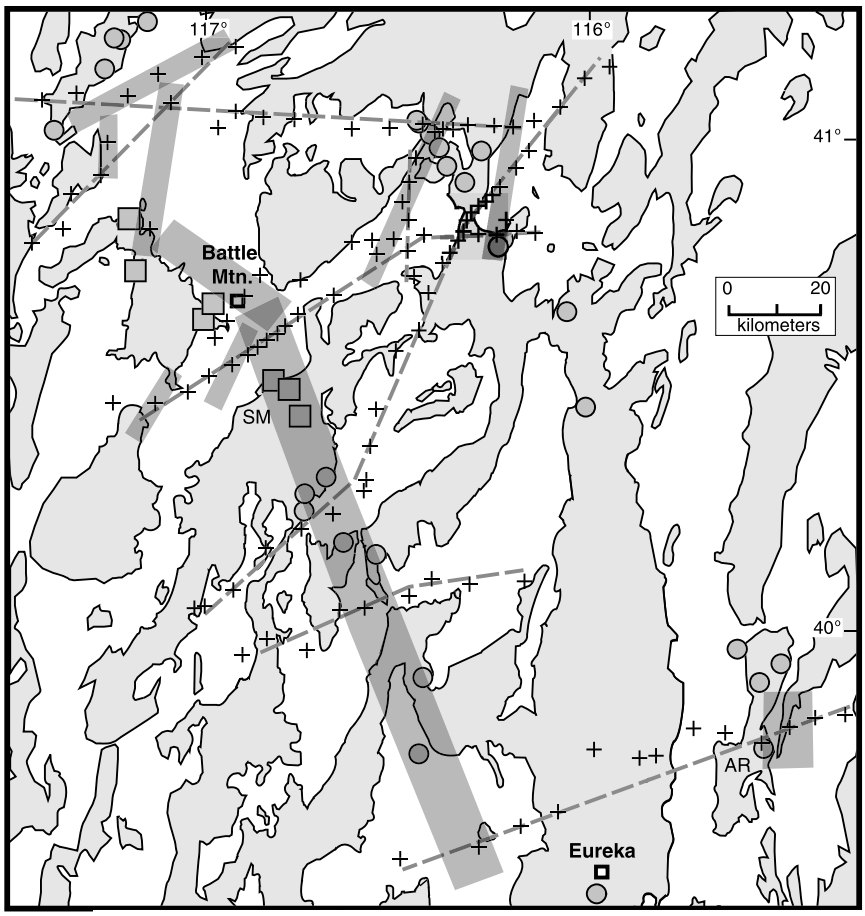

FIG. 6. Location of magnetotelluric transects, stations, and interpreted crustal fault zones from Rodriguez and Williams (2002). Area located on Figure 1. Deposits (gray circles and squares) and ranges (shaded areas) from Figure 1. Magnetotelluric stations (+) were modeled along profiles (dashed lines). Crustal fault zones (semitransparent, dark gray swaths) are inferred where two-dimensional, nearly vertical, deeply penetrating electrical conductors were required by the models. The modeled conductors extend vertically from 1 to 5 km to 18 to 20 km below the surface. Orientations of the crustal fault zones are from estimates of strikes from the magnetotelluric data at 10 km depth. The conductors along the Battle Mountain-Eureka trend are connected into one crustal fault zone that is 10 km wide and about 130 km long. AR = Alligator Ridge deposit and SM = northern Shoshone Mountains (discussed in text).

The two-dimensional conductors located along the Battle Mountain-Eureka trend from just south of Battle Mountain to the latitude of Eureka can be connected to form a zone approximately 130 km long and 10 km wide (Fig. 6), providing important evidence for a crustal fault zone located along the Battle Mountain-Eureka trend (Grauch et al., 2003). At the northern end of the Battle Mountain-Eureka trend, from southwest of Battle Mountain to immediately south of the Getchell trend, the shorter segments of two-dimensional conductors with multiple orientations (Fig. 6) indicate greater structural complexity. North-northwest– to west-northwest–striking, deeply rooted structural zones in the Battle Mountain mining district (Hildenbrand et al., 2001) suggest that the structural complexity may be even greater in detail.

Two-dimensional conductors are oriented oblique to the Carlin mineral trend and its associated isotopic boundary (Fig. 6) near the main part of the trend and near the Alligator Ridge deposit (AR in Fig. 6), which some workers consider a southern extension of the Carlin trend (Nutt et al., 2000). The oblique orientations of the crustal fault zones suggest a lack of control by the western edge of the Precambrian continental crust. The easternmost inferred crustal fault zone within the Carlin trend near 41° N, 116° W (Fig. 6) roughly corresponds to the northern part of the Crescent Valley-Independence lineament recognized from the alignment of geologic and surface features (Peters, 1998). The north-south fault zone near the Alligator Ridge deposit fits with a regional fault zone indicated by geologic mapping (Nutt et al., 2000).

Synthesis

Lines drawn along selected ridges from the HGM maps (Figs. 4d and 5d), which represent the general locations of density and magnetic boundaries, respectively, are overlain with the isotopic province boundaries on Figure 7. The gravity and magnetic boundaries delineate abrupt physical-property contrasts, whereas the isopleths of Sr and Pb isotope ratios mark transitions in crustal composition that are likely gradational. The linearity of the geophysical boundaries over

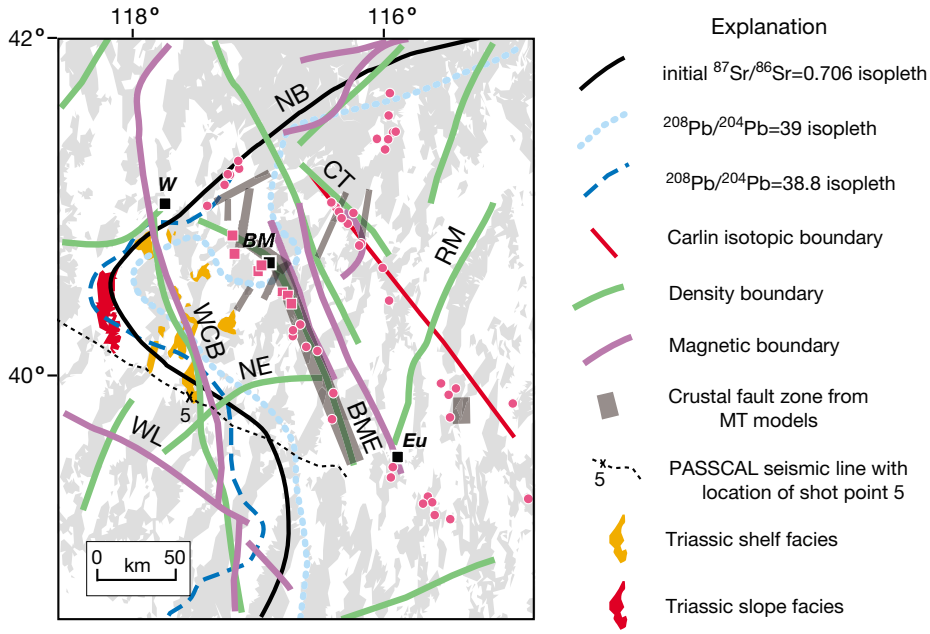

FIG. 7. Compilation of the locations of density and magnetic boundaries (Fig. 4d and 5d), interpreted crustal fault zones from magnetotelluric data (Fig. 6), and isotopic province boundaries (Fig. 2). Density and magnetic boundaries were drawn along selected ridges from their respective horizontal-gradient magnitude maps (Figs. 4d and 5d). Seismic-refraction models from PASSCAL data (Catchings, 1992) indicate an abrupt eastward thickening of upper and lower crust about 10 km southeast of shot point 5 (marked X). The transition between mapped shelf (orange) and slope (red) facies marks the stratigraphic edge of the continent during Triassic time, which generally formed in the same position as the Paleozoic stratigraphic edge (Elison et al., 1990). BME = Battle Mountain-Eureka trend, CT = Carlin trend, NB = northern boundary of continental and transitional crust, RM = Ruby Mountains, WCB = west-central boundary, WL = Walker Lane.

great extent, the common coincidence of density and magnetic boundaries, and the magnetotelluric evidence of a crustal fault zone along part of the Battle Mountain-Eureka trend combine to suggest that many of the boundaries represent crustal fault zones. Many of the boundaries are also associated with the Precambrian rift-related and transform faults inferred from the isotopic province boundaries (Tosdal et al., 2000), suggesting a Precambrian origin. Alternatively, some of the geophysical boundaries may have originated from continental margin modification in middle or late Paleozoic time.

Boundaries related to mineral trends

The Carlin boundary generally coincides with a regional contrast in isotopic character that is inferred as the edge of Precambrian continental crust (Tosdal et al., 2000), a density boundary, and part of a curvilinear magnetic boundary (CT, Fig. 7). The density boundary is apparent in Bouguer gravity data (Fig. 4d), but it is difficult to determine from gravity maps that have been filtered to remove the effects of sources below the upper crust (Grauch et al., 1995; Hildenbrand et al., 2000). This difficulty implies that the density contrast arises from deep sources, such as the difference in crustal composition across the continental edge, rather than from a juxtaposition of dissimilar rock types in the overlying upper crustal rocks. Magnetotelluric evidence (Fig. 6) suggests that faults in the upper crust near the Carlin trend are not related to the continental margin. On the other hand, geologic studies indicate that the deep continental edge influenced upper crustal rocks through long-lived fluid migration (Hofstra and Cline, 2000) and a regional, northwest-trending zone of crustal weakness aligned with the Carlin trend (Teal and Jackson, 1997).

The curvilinear magnetic boundary may arise from the contrast in magnetic properties between sedimentary and igneous rocks in the upper crust. At the southern part of the Carlin mineral trend, the magnetic boundary wraps around the southern end of a teardrop-shaped magnetic high attributed to a Mesozoic-Tertiary intrusive complex (Fig. 5a; Grauch, 1996).

Unlike the isotopic boundary aligned with the Carlin trend that extends southeastward to at least longitude 115° W, the associated density boundary is limited in extent (CT in Fig. 7). In fact, a northeast-trending density boundary (RM in Fig. 7) apparently crosses the isotopic boundary at about 115° 45' W, 40° 15' N. Its strong expression in the HGM map (Fig. 4d) may mask the expression of the southeastern extension of the Carlin boundary. The northeasterly boundary runs along the northwestern side of the Ruby Mountains and coincides with the western limit of a large region in eastern Nevada that underwent high-magnitude extension in early Tertiary time (Seedorff, 1991; Wernicke, 1992).

The Battle Mountain-Eureka boundary is associated with a density boundary (BME in Fig. 7), a contrast in isotopic character (Fig. 3), and a zone of major, nearly vertical electrical conductors south of Battle Mountain, as indicated by the magnetotelluric models (Figs. 6 and 7). As noted by John et al. (2000), unfiltered gravity anomalies show greater correspondence with the Northern Nevada rift than the Battle Mountain-Eureka trend, especially north of Battle Mountain

(Fig. 4a). However, this expression is subordinate to the regional gradient evident from gravity data filtered to enhance the deep sources (Fig. 4c) and from gravity models (Grauch et al., 2003). The density boundary (BME in Fig. 7), which corresponds to the regional gravity gradient, follows the Battle Mountain-Eureka mineral trend more closely than it follows the Northern Nevada rift, from northwest of Battle Mountain to Eureka (Fig. 7). South of Eureka, the density boundary is less evident and diverges from the alignment of mineral deposits (Fig. 4d).

Gravity models, constrained by geologic and other geophysical information, suggest that the regional contrast in density across the central part of the Battle Mountain-Eureka trend arises from the juxtaposition of primarily carbonate rocks intruded by Mesozoic intermediate-composition rocks on the northeast against clastic rocks intruded by Tertiary silicic igneous rocks on the southwest (Grauch et al., 2003). The difference in sedimentary rock type probably originally developed at the edge of the continental shelf along the Precambrian rift-related or transform fault, but it was later enhanced by intrusion of magma of different density and sharpened by subsequent faulting. Regional geochemical anomalies in stream sediment and soil samples also follow the Battle Mountain-Eureka trend from Battle Mountain to the latitude of Eureka (Ludington et al., 2000; Mihalasky, 2000), suggesting that the fault zone associated with the Battle Mountain-Eureka boundary guided regional-scale circulation of hydrothermal fluids at some time in the past. Northwest of Battle Mountain, the gravity data are interpreted as a single boundary (Fig. 7). However, crustal faults interpreted from magnetotelluric models (Fig. 6) and district-scale gravity and magnetic interpretations (Hildenbrand et al., 2001) indicate that several fault zones with multiple orientations may be present in the area.

Massengill (2001) suggested that more than 80 km of right-lateral displacement has occurred along the Battle Mountain-Eureka trend during Tertiary time. If so, large-scale strike-slip faulting should be more apparent at the surface, analogous to the well recognized transverse faults in the Walker Lane belt (Stewart, 1988). The faulting should be especially apparent in the area of Shoshone Mountain (SM in Fig. 6), where magnetotelluric models indicate that the crustal fault zone is present 1 to 3 km below upper-plate rocks of the Roberts Mountains allochthon (Rodriguez and Williams, 2001, 2002). However, no major northwest-striking fault is obvious at the surface here, suggesting that major lateral movement on the Battle Mountain-Eureka boundary had ceased soon after the allochthon was emplaced.

The magnetic boundary just to the east of the density boundary associated with the Battle Mountain-Eureka trend (BME in Fig. 7) is related primarily to the Northern Nevada rift, which may have been partially controlled by the older structure (John et al., 2000). The expression of the deep magmatic roots of the Northern Nevada rift dominates the magnetic signature between the Carlin and Battle Mountain-Eureka boundaries (Fig. 5c). The linearity of the magnetic boundaries defining the sides of these roots (Figs. 5d and 7) suggests that these are faults bounding the Northern Nevada rift at depth. They may also be original Precambrian rift or transform faults owing to their northwest trends.

The Independence Mountains and Getchell trend deposits are located near the $Sr_{initial}$ = 0.706 isopleth, along the northeast-trending boundary of the inferred Precambrian crust (NB in Fig. 7). Density and magnetic boundaries of limited extent occur along the northeastern portion of this boundary, but not near the deposits themselves. The northeast-trending magnetic boundary (NB in Fig. 7) marks the northwestern limit of the area of low magnetic potential, and it locates the division between dominantly oceanic lower to middle crust on the northwest and continental and transitional crust on the southeast, as discussed earlier.

A structural boundary in west-central Nevada

The $Sr_{initial}$ = 0.706 and analogous Pb isotope isopleths generally snake around north-northwest–trending, coincident magnetic and density boundaries from about 41° N, 118° W to 39°, 117° W (WCB in Fig. 7). The magnetic boundary is an expression of a steep increment in the gradual increase of magnetic potential values from east to west (Fig. 5c). The coincidence of the density and magnetic boundaries, their linearity, and their location near the isopleths of Sr and Pb isotope ratios and limit of the area of low magnetic potential values suggest that this is a structural boundary related to the margin of the Precambrian crust. The boundary coincides with the stratigraphically defined continental edge of Elison et al. (1990) that occurs between mapped Triassic slope and shelf facies (Fig. 7) from about 41° to 39°30' N latitude. Elison et al. (1990) considered the stratigraphically defined continental edge to be located at the suture between the Precambrian crust and the Paleozoic arc (Sonomia) that was accreted in Late Permian to Early Triassic time. They suggest that vertical movement occurred along the suture zone as accretion stresses relaxed, accompanied by basaltic volcanism. An abrupt eastward thickening of both the upper and lower crust evident from a model of the PASSCAL seismic refraction profile corresponds with the $Sr_{initial}$ = 0.706 isopleth (Catchings, 1992) and the west-central density and magnetic boundary where the profile crosses the boundary about 10 km southeast of shot point 5 (Fig. 7). The vertical movement postulated by Elison et al. (1990) would have resulted in an increase in crustal thickness on the east side, which fits the seismic-refraction model to the south. Alternatively, the increase in thickness may be related to accommodation of Tertiary extension (Catchings, 1992), which is more likely expressed in the Bouguer gravity data by the northeast-trending regional gradient that extends from the southwest corner of the study area (NE in Fig. 7) to its north-central edge (Fig. 4b and c). The northeast gradient is primarily due to deep-seated masses that presently compensate for the regional differences in elevation across the Basin and Range province, as indicated by isostatic regional gravity fields modeled for the region (Saltus, 1988; Ponce, 1997; Grauch et al., 2003; Fig. 2). The gradient crosses the isotopic isopleths in the southwestern part of the study area (NE in Fig. 7) but follows them in the northeastern part (NB in Fig. 7), suggesting that it is a young feature that is partially controlled by older structures.

The west-central boundary likely originated as part of the Precambrian rift system, similar to the fault zones associated with the Carlin and Battle Mountain-Eureka boundaries. It may have later controlled the emplacement of magma related

to the alignments of the magnetic anomalies subparallel to the Northern Nevada rift (E and W in Fig. 5b), which lie west of the west-central boundary (cf. WCB in Figs. 5b and 7). This magma likely intruded during mid-Miocene time and may be associated with epithermal precious-metal mineralization (Ponce and Glen, 2002). On the other hand, the west-central boundary is apparently not associated with an alignment of Carlin-type deposits (Fig. 7).

The west-central boundary is interrupted by the west-northwest–trending boundary that marks the magnetically defined northeastern limit of the Walker Lane tectonic region (WL in Fig. 7). The magnetically defined limit of the Walker Lane parallels but is to the northeast of the geologically defined Walker Lane belt (Blakely, 1988). The high magnetic values in this region can be explained by pervasive igneous intrusions in the dominantly oceanic crust that were emplaced during construction of Mesozoic magmatic arcs (Stewart, 1980; Blakely, 1988; Hildenbrand et al., 2000).

The basic crustal structure

A simplified view of the crustal structure of probable Precambrian to Triassic age is shown in present-day configuration in Figure 8a. Continental, transitional, and dominantly oceanic ("oceanic") crust was determined somewhat subjectively from the isotopic and geophysical constraints. The region of continental crust was determined primarily from the eastern isotopic province (Fig. 2). The isotopic boundary along the Carlin trend is the primary guide for the southwestern boundary (CT in Fig. 8a). The northwestern boundary of the continental crust is defined by the near coincidence of the $Sr_{initial}$ = 0.706 isopleth and density and magnetic boundaries (NB in Fig. 7).

The central province (Fig. 2), combined with the area of low magnetic potential values (Fig. 5c), was used to define the region of transitional crust; note that the low magnetic potential values gradually increase westward toward more oceanic crust. The transitional crust is bounded by the Carlin boundary on the northeast and the west-central boundary on the west (CT and WCB in Fig. 8a). The transitional crust is further divided by the dominance of continental (c > o) versus oceanic (o > c) components (Fig. 8a), which is inferred from the isotopic character across the Battle Mountain-Eureka trend (Fig. 3). An area of high-density upper crust (Fig. 8a) generally corresponds with the transitional crust with greater continental components. This area was drawn from the promontory in the gravity map of Figure 4c between the Carlin and Battle Mountain-Eureka boundaries. It has also been generally recognized in gravity data filtered to isolate density variations in the upper crust (Hildenbrand et al., 2000).

The edges of the promontory that compose the northwestern boundary of the transitional crust (bold dashed line in Fig. 8a) are not well defined. The continental margin here is inferred to be along the northern limit of low magnetic potential values (Fig. 5c) rather than along the $Sr_{initial}$ = 0.706 isopleth. The low magnetic-potential values suggest the absence of oceanic crust. In addition, the boundary is not drawn along the prominent north-trending magnetic boundary extending north from the west-central boundary (WCB in Fig. 7), because this part of the magnetic boundary is likely related to a Tertiary feature (Fig. 8d).

The boundary of the western province (Fig. 2), combined with moderate to very high magnetic potential values, was used to determine the regions of dominantly oceanic crust. This crust likely produces only moderately high magnetic values. The highest magnetic values probably result from the combined effects of the dominantly oceanic crust plus the effects of pervasive igneous intrusions emplaced in the upper crust during Mesozoic and Tertiary time.

An anomalous radiogenic area discussed by Tosdal et al. (2000) is included in the picture of the crustal structure (Fig. 8a). The East Range block has unusually radiogenic Pb and Sr isotope compositions and is located in the northeastern corner of the $Sr_{initial}$ = 0.706 isopleth. Tosdal et al. (2000) considered this radiogenic block to indicate an area of thicker crust that is out of place with respect to its location near the edge of the continent. The block suggests that significant lateral movement of the crust occurred along the continental margin during or after Precambrian rifting.

Implications for Tectonic History

Combining tectonic elements of successively younger ages to the picture of the basic crustal structure helps elucidate the influence of the older structure on the younger events. Each illustration of Figure 8 represents the present-day configuration of the tectonic elements of the ages noted. The elements may have moved from their original positions relative to each other, but our constraints are not sufficient to attempt a palinspastic restoration. Because of the tectonic complexity and many controversies involved in the interpretation of the tectonic history, the figures are simplified and many major tectonic elements are not shown. A detailed discussion of the range of interpretations and problems with the tectonic elements shown is beyond the scope of this paper.

The basic crustal structure (Fig. 8a) was established as early as Neoproterozoic time, after Rodinia had rifted apart and a passive margin was established at the western edge of the continent. The northwest-striking fault zones (CT, BME, and WCB in Fig. 8a) were likely part of the Precambrian rift system. Alternatively, some of these boundaries may have developed during the Antler and/or Sonoma orogenies (Fig. 8b) as sutures or strike-slip accommodation of oblique plate-margin stresses, as suggested by Jones (1991) and discussed by Crafford and Grauch (2002). The west-central boundary, in particular, may represent the Triassic suture of Elison et al. (1990), along which the arc was accreted during the Sonoma orogeny. The large, clastic Antler foreland basin (Fig. 8b), which developed east of the eastern limit of the Roberts Mountains allochthon after the Antler orogeny, crosses the southern extension of the Carlin boundary. This large pile of low-density sedimentary rock may be a significant contributor to the gravity low in the area (Fig. 4c) that obscures the gravity signature of the Carlin boundary.

A transition from less dense limestone- and shale-dominated assemblages in the southwest to denser, dolomite-dominated assemblages on the northeast was generally located near the Battle Mountain-Eureka trend area throughout Paleozoic time (Matti and McKee, 1977; Stewart, 1980; Poole et al., 1992). The difference in sedimentary rock types may partially explain the density contrast in the upper crust at the

Battle Mountain-Eureka trend (Grauch et al., 2003). Rheologic differences resulting from the lithologic contrasts across the Battle Mountain-Eureka boundary may have controlled the emplacement of the Roberts Mountains allochthon in Mississippian time (Figure 8b). The dolomite assemblage rocks may have acted as a buttress to thrust packages moving eastward, forcing them to ramp up and create the Antler highland, which was located east of the Battle Mountain-Eureka boundary (Stewart, 1980; Miller et al., 1992).

In Jurassic to Early Cretaceous time, intense folding and thrusting was concentrated in the old Antler foreland basin and in accreted terrane outboard of the continental crust (Fig. 8c). Large-scale shearing was initiated in the Walter Lane belt (Stewart, 1988). The Carlin and Battle Mountain-Eureka boundaries likely influenced Jurassic folds with northwest-trending axes concentrated in the region between the Carlin and Battle Mountain-Eureka trends (Fig. 8c; Madrid and Roberts, 1991) and Mesozoic granitic rocks (not shown) that were emplaced along the mineral trends (Madrid and Roberts, 1991; Shawe, 1991).

The tectonic elements of Late Cretaceous to Oligocene age reflect a change from contractional to extensional regimes. Blakely and Jachens (1991) suggested that voluminous silicic magmatism in a curved belt southwest of the Battle Mountain-Eureka trend (Fig. 8d) gave rise to lower gravity values in this area (cf. Figs. 4b and 8d). Large-magnitude extension was generally concentrated within distinct domains (Fig. 8e). In particular, the area of the old Antler foreland basin includes metamorphic core complexes like the Ruby Mountains (Wernicke, 1992). This deformation could have obliterated the physical signature of older structures and lithologic contacts in the upper crust, such as the Carlin boundary. During this time, regional hydrothermal fluid flow deposited metals along the mineral trends and in other isolated deposits (Maher et al., 1993; Hofstra et al., 1999). The Carlin and Battle Mountain-Eureka boundaries may have acted as general pathways by which deep-origin hydrothermal fluids interacted with meteoric waters in the upper crust, whereas younger, shallow structures and lithologic variations served to focus fluid flow and mineralization at a local scale (e.g., Shawe, 1991; Hofstra and Cline, 2000).

In Miocene time, magmatism was concentrated in the northern part of the area (Fig. 8d), except for the Northern Nevada rift (John et al., 2000) and inferred mafic intrusions forming the subparallel magnetic anomalies to the west (Fig. 8f). The magmas of the Northern Nevada rift may have reoccupied fractures and faults related to the Battle Mountain-Eureka boundary only between Battle Mountain and Eureka, which would explain the divergence of the rift north of Battle Mountain (Fig. 8f). Intrusions related to the subparallel magnetic anomalies may have used fractures and faults related to the west-central boundary (WCB in Fig. 8a and 8f).

Selected tectonic elements developed from Miocene time to present are shown in Figure 8f. Some disruption of the direction or continuity of ranges is evident (but not conspicuous) where the northwest striking structures are located. The concentration of modern-day seismicity in the Central Nevada seismic belt falls mostly west of the west-central boundary within the old accreted terrane (Fig. 8b).

The most remarkable part of the present-day picture is the continuity of the crustal fault zones. Their early Mesozoic or older ages are determined by the associated contrasts in isotopic character that were in place by Jurassic time. As argued by Wooden et al. (1998) and Tosdal et al. (2000), the most likely tectonic event that shaped such crustal features occurred during the Neoproterozoic breakup of Rodinia. Alternatively, they may have originated during late Paleozoic or Triassic continental margin modification. The linear geophysical boundaries that are spatially related to the contrasts in isotopic character can not be merely a coincidence. We conclude that these geophysical signatures represent the final products of millions of years of reactivation or influence of the fault zones throughout the Phanerozoic.

Conclusions

We combined information from Sr and Pb isotope data (Wooden et al., 1998; Tosdal et al., 2000) and models of recently collected magnetotelluric data (Rodriguez and Williams, 2001, 2002) to develop a new magnetic and gravity interpretation of the crustal structure of north-central Nevada to better understand the origin of mineral trends. Magnetic expression of the crust and abrupt gradients in gravity and magnetic data, where boundaries occur in crustal density and magnetization, are associated with isotopic patterns. Models of magnetotelluric data across one of these boundaries shows that it is a crustal fault zone. We conclude that the geophysical boundaries are present-day expressions of the products of reactivation and/or influence of the older crustal fault zones through time and that the broad character of the magnetic data is an expression of the Precambrian crystalline crust.

On the basis of our comparisons of the isotopic and geophysical data, we developed a simplified view of the crustal structure (Fig. 8a). The portrayal is based on the following conclusions about individual elements.

1. The Carlin mineral trend follows the Carlin boundary, a crustal discontinuity that is primarily defined by a contrast in isotopic character of the crust. The contrast in isotopic character indicates that continental crust is juxtaposed against crust containing significantly more oceanic material. A density boundary follows part of the isotopic boundary and probably arises from a density contrast within the lower to middle crust. The linear portion of a magnetic boundary associated with the contact of an intrusive complex adjacent to the Carlin boundary suggests that magmatism was controlled by the location of the crustal fault. The geophysical expression of the Carlin boundary is terminated by a northeast-trending density boundary that coincides with the western limit of large-magnitude Tertiary deformation. Magnetotelluric models indicate that crustal fault zones near the trend are oblique to it, suggesting these faults were not influenced by the deeper boundary.

2. The Battle Mountain-Eureka mineral trend follows the Battle Mountain-Eureka crustal fault zone, which is primarily defined by a density boundary in the upper crust and a zone of major, nearly vertical, electrical conductors evident from magnetotelluric models. It also corresponds to a subtle contrast in isotopic character that is more pronounced at the northern end of the trend. The crust between the Carlin and

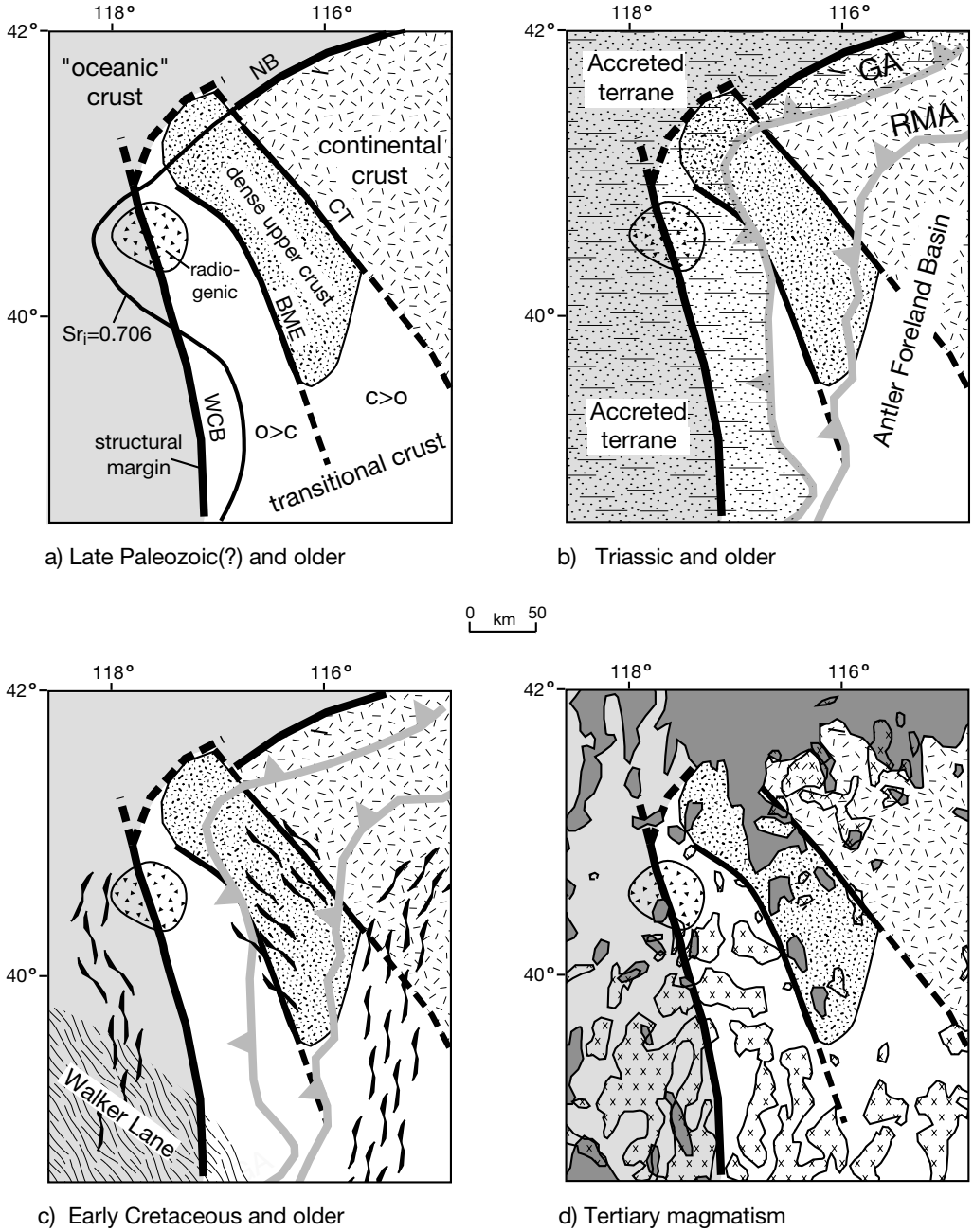

FIG. 8. Present-day configuration of crustal structure overlain by tectonic elements of successively younger ages. Refer to the legend for explanation of the patterns and symbols. a. Basic crustal structure derived from the geophysical boundaries, isotopic patterns, and the magnetic potential map (see text). The structural boundary of the continent is defined from the geophysical boundaries and the limits of the region of low values in the magnetic potential map; it is dashed where it follows the magnetic potential map only. The $Sr_{initial}$ = 0.706 isopleth from Figure 2 may represent gradational, poorly resolved, or displaced variations in the crustal composition in relation to the structural boundary (see text). b. Tectonic elements present by Triassic time, showing the eastern limits of allochthons (RMA and GA), the Antler foreland basin east of the Roberts Mountains allochthon, and associated accreted terranes (from Stewart, 1980). Paleozoic rifting events are not represented. c. Tectonic elements present by Early Cretaceous time, showing belts of folding and thrusting from Cowan and Bruhn (1992) and Madrid and Roberts (1990), and the magnetically defined Walker Lane belt (Blakely, 1988). Limited intrusive activity not represented. d. Tertiary magmatism from Stewart and Carlson (1976), showing silicic volcanic rocks of 43 to 17 Ma and primarily intermediate to mafic volcanic rocks of 17 to 6 Ma. e. Tectonic elements present by Oligocene time, showing regions of large-magnitude extension from Wernicke (1992) and Seedorff (1991) and gold deposits from Figure 1. Extension in the southeastern part of the map may have obliterated the geophysical signature of the southern Carlin boundary. f. Selected tectonic elements present today. The mid-Miocene Northern Nevada rift (NNR) is defined as in Figure 1. The subparallel magnetic anomalies (Fig. 5b) represent buried intrusions that partially parallel the Battle Mountain-Eureka and west-central boundaries, respectively. The Central Nevada seismic belt and locations of historic earthquakes with >6 magnitude are from Rogers et al. (1991).

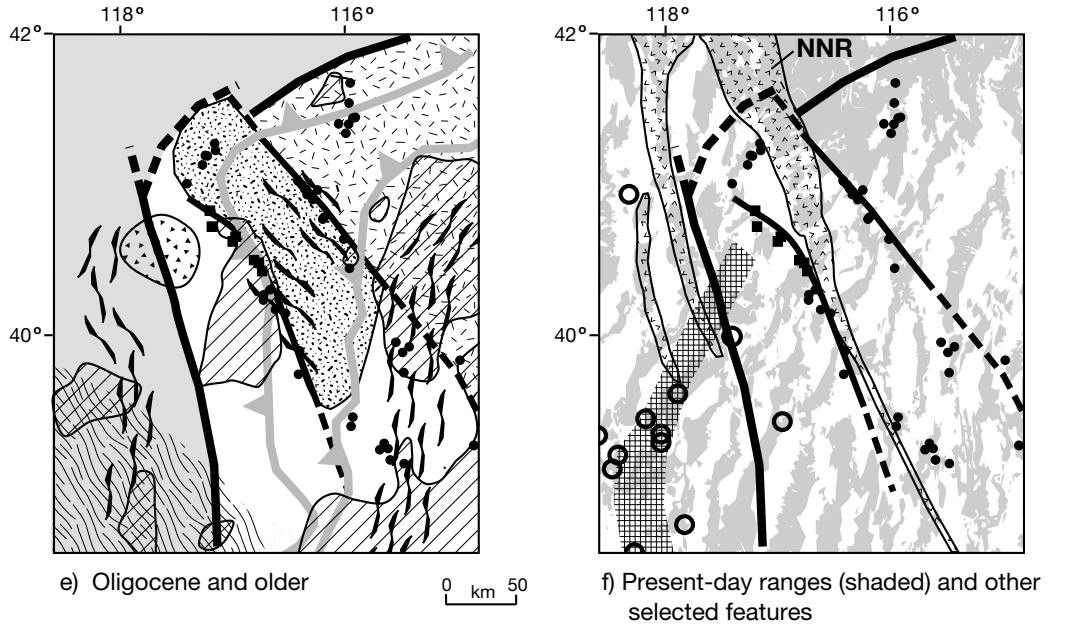

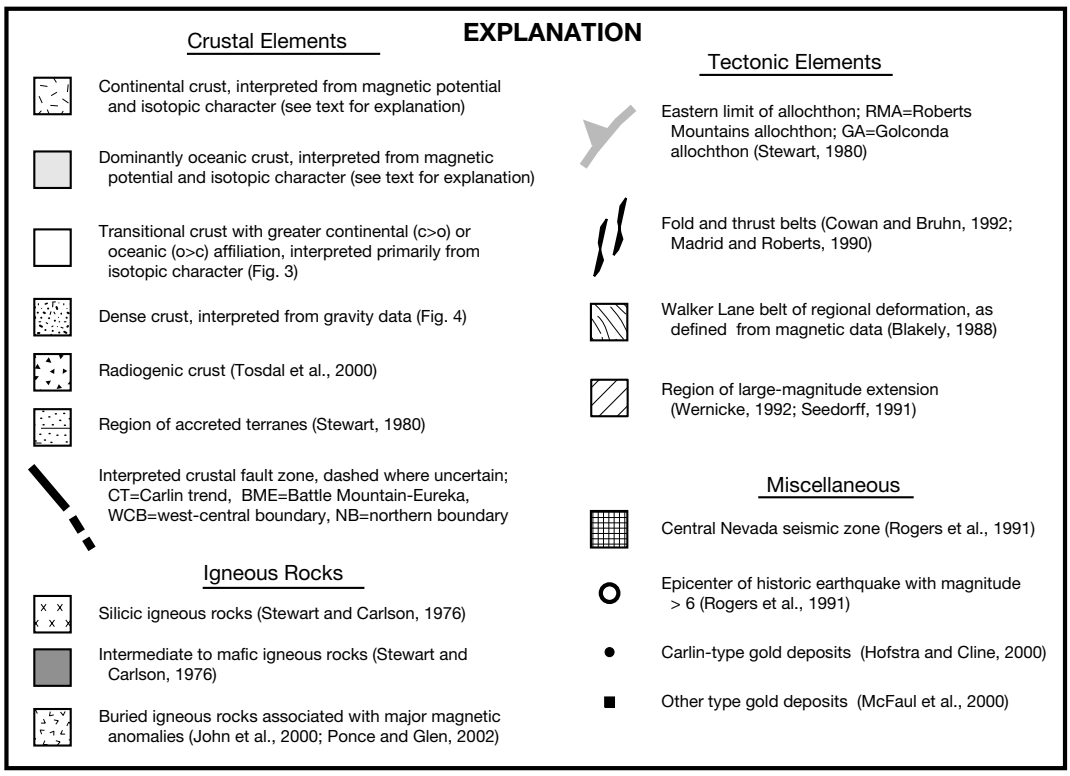

FIG. 8. *(Cont.)*

Battle Mountain-Eureka trends is intermediate in composition between the continental crust east of the Carlin trend and the transitional, more oceanic crust west of the Battle Mountain-Eureka crustal fault zone. Grauch et al. (2003) investigated the nature of the Battle Mountain-Eureka crustal fault zone using gravity and magnetotelluric models. They suggest that the density contrast in the upper crust is due to differences in both sedimentary lithology and the composition of igneous intrusions and later fault displacement near the transition. The magnetotelluric profile models require deeply penetrating, subvertical conductors along the Battle Mountain-Eureka trend that are indicative of large-scale fault zones. A single crustal fault zone about 10 km wide and 130 km long along the Battle Mountain-Eureka trend can be inferred by connecting the locations of the conductors. Near and northwest of Battle Mountain, the crustal fault zones inferred from the magnetotelluric models have multiple orientations, indicating a greater structural complexity.

3. The Independence Mountains and Getchell trend deposits are located near the 0.706 isopleth of initial $^{87}Sr/^{86}Sr$ ratios along the northeast trending, northern boundary of the inferred Precambrian crust. Density and magnetic boundaries follow the isopleth for a limited extent but are not located near the deposits. The proximity of the deposit clusters to the continental margin suggests a genetic relation, but individual crustal structures that may have controlled their distribution are not obvious.

4. A north-northwest–trending structural boundary in west-central Nevada is spatially associated with the isotopically defined, western continental margin and linear magnetic anomalies, similar to the one associated with the Northern Nevada rift. Its significance as a structure related to the continental margin has not been previously recognized. The boundary is identified primarily by coincident magnetic and density boundaries arising from regional gradients. It coincides with the stratigraphically defined Triassic continental edge of Elison et al. (1990) on the north and perhaps with an abrupt increase in upper and lower crustal thickness based on seismic refraction data (Catchings, 1992) on the south. The boundary is probably a crustal fault zone or suture that bounds the western edge of the buried continent. Two linear magnetic anomalies parallel the west-central boundary to the west. The anomalies may be due to mid-Miocene, magma-filled, large-scale fractures (Glen and Ponce, 2002) that may be related to epithermal precious-metal deposits (Ponce and Glen, 2002) and were probably controlled by the older fault zone. Unlike the Carlin and Battle Mountain-Eureka boundaries, the west-central boundary is apparently not associated with an alignment of Carlin-type gold deposits.

5. Low values of magnetic potential data (magnetic data filtered to enhance very broad features) correspond well with the limits of the Precambrian crystalline crust as defined by $Sr_{initial}$ = 0.706 and indicate that basement rocks have low magnetization. The low magnetization is most likely due to magnetite-poor crystalline rocks rather than a shallow Curie isotherm that causes basement rocks to lose their magnetization. Thus, we used the regions of low magnetic potential to define the limits of the Precambrian crystalline crust. Magnetic values gradually increase toward the continental margin, corresponding with the increase in mafic material predicted from the isotopic data.

Comparing this view of crustal structure with tectonic elements of successively younger ages shows that the rift margins and fault zones developed during Precambrian rifting and/or later continental margin modification have had a profound influence on many subsequent tectonic events. These events include sedimentation, deformation, magmatism, extension, and most important, mineralization. During compressional events, discontinuities at the fault zones may have acted as buttresses that controlled allochthon emplacement or folding, or the faults may have reactivated as thrust or strike-slip faults. During extensional events, the fault zones guided rifting, magmatism, and fluid flow. The continuity of the fault zones today implies that they have influenced the Tertiary breakup of the crust, suggesting that large blocks of crust have remained fairly intact between regions of deformation. In short, the geophysical signatures of the crustal fault zones reflect the final products of millions of years of reactivation and/or influence of the fault zones throughout the Phanerozoic.

Acknowledgments

This paper has significantly improved as a result of reviews by Liz Crafford, Jeff Doebrich, Tom Hildenbrand, Dave John, Bob Karlin, James Wright, and Mark Hannington.

REFERENCES

Baranov, V., 1957, A new method for interpretation of aeromagnetic maps—Pseudogravity anomalies: Geophysics, v. 22, p. 359–383.

Blakely, R.J., 1988, Curie temperature isotherm analysis and tectonic implications of aeromagnetic data from Nevada: Journal of Geophysical Research, v. 93, p. 11,817–11,832.

——1995, Potential theory in gravity and magnetic applications: New York, Cambridge University Press, 441 p.

Blakely, R.J., and Jachens, R.W., 1991, Regional study of mineral resources in Nevada: Insights from three-dimensional analysis of gravity and magnetic anomalies: Geological Society of America Bulletin, v. 103, p. 795–803.

Blakely, R.J., and Simpson, R.W., 1986, Locating edges of source bodies from magnetic and gravity anomalies: Geophysics, v. 51, p. 1494–1496.

Burchfiel, B.C., Cowan, D.S., and Davis, G.A., 1992, Tectonic overview of the Cordilleran orogen in the western United States, *in* Burchfiel, B.C., Lipman, P.W., and Zoback, M.L., eds., The Cordilleran orogen: Conterminous U.S.: Geological Society of America, The Geology of North America, v. G-3, p. 407–479.

Catchings, R.D., 1992, A relation among geology, tectonics, and velocity structure, western to central Nevada Basin and Range: Geological Society of America Bulletin, v. 104, p. 1178–1192.

Christiansen, R.L., and Yeats, R.S., *with contributions by* Graham, S.A., Niem, W.A., Niem, A.R., and Snavely, Jr., P.D., 1992, Post-Laramide geology of the U.S. Cordilleran region, *in* Burchfiel, B.C., Lipman, P.W., and Zoback, M.L., eds., The Cordilleran orogen: Conterminous U.S.: Geological Society of America, The Geology of North America, v. G-3, p. 261–406.

Cordell, L., 1979, Gravimetric expression of graben faulting in Santa Fe Country and the Española basin, New Mexico: New Mexico Geological Society Guidebook, 30th Field Conference, p. 59–64.

Cordell, L., and Grauch, V.J.S., 1985, Mapping basement magnetization zones from aeromagnetic data in the San Juan basin, New Mexico, *in* Hinze, W.J., ed., The Utility of Regional Gravity and Magnetic Anomaly Maps: Society of Exploration Geophysicists, Tulsa, Oklahoma, p. 181–197.

Cowan, D.S., and Bruhn, R.L., 1992, Late Jurassic to early Late Cretaceous geology of the U.S. Cordillera, *in* Burchfiel, B.C., Lipman, P.W., and Zoback, M.L., eds. The Cordilleran orogen: Conterminous U.S.: Geological Society of America, The Geology of North America, v. G-3, p. 169–203.

Crafford, A.E.J., and Grauch, V.J.S., 2002, Geologic and geophysical evidence for the influence of deep crustal structures on Paleozoic tectonics and the alignment of world-class gold deposits, north-central Nevada, USA: Ore Geology Reviews, v. 21, p. 157–184.

Dalziel, I.W.D., 1997, Overview: Neoproterozoic-Paleozoic geography and tectonics: Review, hypothesis, environmental speculations: Geological Society of America Bulletin, v. 109, p. 16–42.

Eaton, G.P., Wahl, R.R., Prostka, H.J., Mabey, D.R., and Kleinkopf, M.D., 1978, Regional gravity and tectonic patterns: Their relation to late Cenozoic epeirogeny and lateral spreading in the western Cordillera, *in* Smith, R.B., and Eaton, G.P., eds., Cenozoic tectonics and regional geophysics of the western Cordillera: Geological Society of America Memoir 152, p. 51–91.

Eberhart-Phillips, D., Stanley, W.D., Rodriguez, B.D., and Lutter, W.J., 1995, Surface seismic and electrical methods to detect fluids related to faulting: Journal of Geophysical Research, v. 100, no. B7, p. 12,919–12,936.

Elison, M.W., Speed, R.C., and Kistler, R.W., 1990, Geologic and isotopic constraints on the crustal structure of the northern Great Basin: Geological Society of America Bulletin, v. 102, p. 1077–1092.

Glen, J.M.G., and Ponce, D.A., 2002, Large-scale fractures related to inception of the Yellowstone hotspot: Geology, v. 30, p. 647–650.

Grauch, V.J.S., 1996, Magnetically interpreted, granitoid plutonic bodies in Nevada *in* Singer, D., ed., An analysis of Nevada's metal-bearing mineral resources: Nevada Bureau of Mines and Geology Open-File Report 96-2, p. 7-1 through 7-16, 1 plate, scale 1:1,000,000.

Grauch, V.J.S., and Cordell, L., 1987, Limitations of determining density and magnetic boundaries from the horizontal gradient of gravity and pseudo-gravity data: Geophysics, v. 52, p. 118–121.

Grauch, V.J.S., Jachens, R.C., and Blakely, R.J., 1995, Evidence for a basement feature related to the Cortez disseminated gold trend and implications for regional exploration in Nevada: Economic Geology, v. 90, p. 203–207.

Grauch, V.J.S., Rodriguez, B.D., Bankey, V., and Wooden, J.L., 2003, Evidence for a Battle Mountain-Eureka crustal fault zone, north-central Nevada, and its relation to Neoproterozoic-early Paleozoic continental breakup: Journal of Geophysical Research, v. 108, no B3, 2140, doi: 10.1029/2001JB000681.

Hildenbrand, T.G., and Kucks, R.P., 1988, Total intensity magnetic anomaly maps of Nevada: Nevada Bureau of Mines and Geology Map 93A, scale 1:1,000,000.

Hildenbrand, T.G., Berger, B., Jachens, R.C., and Ludington, S., 2000, Regional crustal structures and their relationship to the distribution of ore deposits in the western United States, based on magnetic and gravity data: Economic Geology, v. 95, p. 1583–1603.

Hildenbrand, T.G., Berger, B., Jachens, R.C., and Ludington, S., 2001, Utility of magnetic and gravity data in evaluating regional controls on mineralization: Examples from the western United States: Reviews in Economic Geology, v. 14, p. 75–109.

Hofstra, A.H., and Cline, J.S., 2000, Characteristics and models for Carlin-type gold deposits: Reviews in Economic Geology, v. 13, p. 163–220.

Hofstra, A.H., Snee, L.W., Rye, R.O., Folger, H.W., Phinisey, J.D., Loranger, R.J., Dahl, A.R., Naeser, C.W., Stein, H.J., and Lewchuk, M., 1999, Age constraints on Jerritt Canyon and other Carlin-type gold deposits in the western United States—Relationship to mid-Tertiary extension and magmatism: Economic Geology, v. 94, p. 769–802.

Jachens, R.C., and Moring, B.C., 1990, Maps of the thickness of Cenozoic deposits and the isostatic residual gravity over basement for Nevada: U.S. Geological Survey Open-File Report 90-404, 15 p., 2 sheets, scale 1:1,000,000.

John, D.A., Wallace, A.R., Ponce, D.A., Fleck, R.B., and Conrad, J.E., 2000, New perspectives on the geology and origin of the Northern Nevada rift, *in* Cluer, J.K., Price, J.G., Struhsacker, E.M., Hardyman, R.F., and Morris, C.L., eds., Geology and Ore Deposits 2000: The Great Basin and Beyond: Geological Society of Nevada Symposium, Reno, 2000, Proceedings, v. 1. p. 127–154.

Jones, A.E., 1991, Sedimentary rocks of the Golconda terrane: Provenance and paleogeographic implications, *in* Cooper, J.D., and Stevens, C.H., eds., Paleozoic paleogeography of the western United States, II: Society of Economic Paleontologists and Mineralogists Pacific Section, p. 783–800.

Karlstrom, K.E., Harlan, S.S., Williams, M.L., McLelland, J., Geissman, J.W., and Åhäll, K-I., 1999, Refining Rodinia: Geologic evidence for the Australia-western U.S. connection in the Proterozoic: GSA Today, v. 9, no. 10, p. 1–7.

Keller, G.V., 1989, Electrical properties, *in* Carmichael, R.S., ed., Practical handbook of physical properties of rocks and minerals: Boca Raton, Florida, CRC Press, p. 359–427.

Kistler, R.W., 1983, Isotope geochemistry of plutons in the northern Great Basin: Davis, California, Geothermal Resources Council Special Report 13, p. 3–8.

Kistler, R.W., and Peterman, Z.E., 1978, Reconstruction of crustal blocks of California on the basis of initial strontium isotopic compositions of Mesozoic granitic rocks: U.S. Geological Survey Professional Paper 1071, 17 p.

Klemperer, S.L., Hauge, T.A., Hauser, E.C., Oliver, J.E., and Potter, C.J., 1986, The Moho in the northern Basin and Range province, Nevada, along the COCORP 40° seismic-reflection transect: Geological Society of America Bulletin, v. 97, p. 603–618.

Levy, M., and Christie-Blick, N., 1989, Pre-Mesozoic palinspastic reconstruction of the eastern Great Basin (western United States): Science, v. 245, p. 1454–1462.

Ludington, S., Folger, H., Hildenbrand, T.G., and Kotlyar, B., 2000, Arsenic distribution in surficial materials of the northern Great Basin [abs.]: Geological Society of America Abstracts with Programs, v. 32, p. A-392.

Mabey, D.R., Zietz, I., Eaton, G.P., and Kleinkopf, M.D., 1978, Regional magnetic patterns in part of the Cordillera in the western United States, *in* Smith, R.B., and Eaton, G.P., eds., Cenozoic tectonics and regional geophysics of the western Cordillera: Geological Society of America Memoir 152, p. 93–106.

Madrid, R.J., and Roberts, R.J., 1991, Origin of gold belts in north-central Nevada: Geology and ore deposits of the Great Basin—Field Trip Guidebook Compendium, v. 2, Geological Society of Nevada Symposium, Reno, p. 927–939.

Maher, B.J., Browne, Q.J., and McKee, E.H., 1993, Constraints on the age of gold mineralization and metallogenesis in the Battle Mountain-Eureka mineral belt, Nevada: Economic Geology, v. 88, p. 469–478.

Massengill, G., 2001, A Tertiary tectonic twist for northern Nevada based on isotopic data, *in* Shaddrick, D.R., Zbinden, E.A., Mathewson, D.C., and Prenn, C., eds., Regional tectonics and structural control of ore: The major gold trends of northern Nevada: Geological Society of Nevada Special Publication 33, p. 111–113.

Matti, J.C., and McKee, E.H., 1977, Silurian and lower Devonian paleogeography of the outer continental shelf of the Cordilleran miogeocline, central Nevada, *in* Stewart, J.H., Stevens, C.H., and Fritsche, A.E., eds., Paleozoic Paleogeography of the Western United States: Pacific Coast Paleogeography Symposium I: Society of Economic Paleontologists and Mineralogists Pacific Section, p. 181–217.

McFaul, E.J., Mason, G.T., Jr., Ferguson, W.B., and Lipin, B.R., 2000, U.S. Geological Survey Mineral Databases-MRDS and MAS/MILS: U.S. Geological Survey Digital Data Series DDS-52.

McKee, E.H., and Blakely, R.J., 1990, Tectonic significance of linear, north-trending anomalies in north-central Nevada [abs.]: Geological Society of Nevada Geology and ore deposits of the Great Basin, Program with Abstracts, p. 49.

Mihalasky, M.J., 2000, The northern Nevada geochemical "V"-trend [abs.]: Geological Society of America Abstracts with Programs, v. 32, p. A-392.

Miller, E.L., Miller, M.M., Stevens, C.H., Wright, J.E., and Madrid, R., 1992, Late Paleozoic paleogeographic and tectonic evolution of the western U.S. Cordillera, *in* Burchfiel, B.C., Lipman, P.W., and Zoback, M.L., eds., The Cordilleran orogen: Conterminous U.S.: Geological Society of America, The Geology of North America. v. G-3, p. 57–106.

Nettleton, L.L., 1971, Elementary gravity and magnetics for geologists and seismologists: Society of Exploration Geophysicists Monograph 1, 121 p.

North American Magnetic Anomaly Group, 2002, Digital data grids for the magnetic anomaly map of North America: U.S. Geological Survey Open-File Report 02-414, USmag_origmrg.grd available from ftp://musette.cr.usgs.gov/pub/open-file-reports/ofr-02-0414.

Nutt, C.J., Hofstra, K.S., and Mortensen, J.K., 2000, Structural setting and genesis of gold deposits in the Bald Mountain-Alligator Ridge area, east-central Nevada, *in* Cluer, J.K., Price, J.G., Struhsacker, E.M., Hardyman, R.F., and Morris, C.L., eds., Geology and Ore Deposits 2000: The Great Basin and Beyond: Geological Society of Nevada Symposium, Reno, 2000, Proceedings, p. 513–537.

Peters, S.G., 1998, Evidence for the Crescent Valley-Independence lineament, north-central Nevada, *in* Tosdal, R.M., ed., Contributions to the gold metallogeny of northern Nevada: U.S. Geological Survey Open-File Report 98-338, p. 106–118.

Ponce, D.A., 1997, Gravity data of Nevada, U.S. Geological Survey Digital Data Series DDS-42, CD-ROM.

——2003, Geophysical methods and application, *in* Wallace, A.R., Ludington, Steve, Mihalasky, M.J., Peters, S.G., Theodore, T.G., Ponce, D.A., John, D.A., and Berger, B.R., *in* Zientek, M.K., Sidder, G.B., and Zierenberg, R.A., eds., Assessment of metallic mineral resources in the Humboldt River basin, northern Nevada: U.S. Geological Survey Digital Data Series, CD-ROM, in press.

Ponce, D.A., and Glen, J.M.G, 2002, Relationship of epithermal gold deposits to large-scale fractures in northern Nevada: Economic Geology, v. 97, p. 3–9.

Poole, F.G., Stewart, J.H., Palmer, A.R., Sandberg, C.A., Madrid, R.J., Ross, Jr., R.J., Hintze, L.F., Miller, M.M., and Wrucke, C.T., 1992, Latest Precambrian to latest Devonian time; development of a continental margin, *in* Burchfiel, B.C., Lipman, P.W., and Zoback, M.L., eds., The Cordilleran orogen: Conterminous U.S.: Geological Society of America, The Geology of North America, v. G-3, p. 9–56.

Roberts, R.J., 1966, Metallogenic provinces and mineral belts in Nevada: Nevada Bureau of Mines Report 13, p. 47–72.

Rodriguez, B.D., and Williams, J.M., 2001, Deep regional resistivity structure across the Battle Mountain-Eureka and Carlin trends, north-central Nevada: U.S. Geological Survey Open-File Report 01-346, 165 p.

——2002, Resistivity structure across the Humboldt River basin, north-central Nevada: U.S. Geological Survey Open-File Report 02-39, 114 p.

Rogers, A.M., Harmsen, S.C., Corbett, E.J., Priestley, K., and dePolo, D., 1991, The seismicity of Nevada and some adjacent parts of the Great Basin, *in* Slemmons, D.B., Engdahl, E.R., Zoback, M.D., and Blackwell, D.D., eds., Geological Society of America, Neotectonics of North America, Decade Map volume: p. 153–184.

Saltus, R.W., 1988, Regional, residual, and derivative gravity maps of Nevada: Nevada Bureau of Mines and Geology Map 94B, scale 1:1,000,000.

Sass, J.H., Blackwell, D.D., Chapman, D.S., Costain, J.K., Decker, E.R., Lawver, L.A., and Swanberg, C.A., 1981, Heat flow from the crust of the United States, *in* Touloukian, Y.S., Judd, W.R., and Roy, R.F., eds., Physical properties of rocks and minerals, New York, McGraw-Hill, p. 503–548.

Seedorff, E., 1991, Magmatism, extension, and ore deposits of Eocene to Holocene age in the Great Basin—Mutual effects and preliminary proposed genetic relationships, *in* Raines, G.L., Lisle, R.E., Schafer, R.W., and Wilkinson, W.H., eds., Geology and Ore Deposits of the Great Basin: Geological Society of Nevada Symposium, Reno, Proceedings, p. 133–178.

Shawe, D.R., 1991, Structurally controlled gold trends imply large gold resources in Nevada, *in* Raines, G.L., Lisle, R.E., Schafer, R.W., and Wilkinson, W.H., eds., Geology and Ore Deposits of the Great Basin: Geological Society of Nevada, Reno, 1991, Proceedings, p. 199–212.

Shuey, R.T., Schellinger, D.K., Johnson, E.H., and Alley, L.B., 1973, Aeromagnetics and the transition between the Colorado Plateau and Basin Range provinces: Geology, v. 1, p. 107–110.

Stewart, J.H., 1980, Geology of Nevada: Nevada Bureau of Mines Geology Special Publication 4, 136 p.

——1988, Tectonics of the Walker Lane, western Great Basin: Mesozoic and Cenozoic deformation in a shear zone, *in* Ernst, W.G., ed., Metamorphism and crustal evolution of the western U.S. (Rubey Volume VII): Englewood Cliffs, New Jersey, Prentice-Hall, p. 683–713.

Stewart, J.H., and Carlson, J.E., 1976, Cenozoic rocks of Nevada—Four maps and brief description of distribution, lithology, age, and centers of volcanism: Nevada Bureau of Mines and Geology Map 52, scale 1:1,000,000.

——1977, Geologic map of Nevada: Nevada Bureau of Mines Geological Map 57, scale 1:1,000,000.

Teal, L., and Jackson, M., 1997, Geologic overview of the Carlin trend gold deposits and descriptions of recent deep discoveries: Society of Economic Geologists Guidebook Series, v. 28, p. 3–37.

Thompson, G.A., and Burke, D.B., 1974, Regional geophysics of the Basin and Range province: Earth and Planetary Science Annual Review, v. 2, p. 213–238.

Thorman, C.H., Ketner, K.B., Brooks, W.E., and Zimmermann, R.A., 1991, Late Mesozoic-Cenozoic tectonics in northeastern Nevada, *in* Raines, G.L., Lisle, R.E., Schafer, R.W., and Wilkinson, W.H., eds., Geology and Ore Deposits of the Great Basin: Geological Society of Nevada Symposium, Reno, 1991, Proceedings, p. 25–45.

Tosdal, R.M., Wooden, J.L., and Kistler, R.W., 2000, Geometry of the Neoproterozoic continental break-up, and implications for location of Nevadan mineral belts, *in* Cluer, J.K., Price, J.G., Struhsacker, E.M., Hardyman, R.F., and Morris, C.L., eds., Geology and Ore Deposits 2000: The Great Basin and Beyond: Geological Society of Nevada Symposium, Reno, 2000, Proceedings, p. 451–466.

Vozoff, K., 1991, The magnetotelluric method, *in* Nabighian, M.N., ed., Electromagnetic methods in applied geophysics, v. 2; Application, parts A and B: Tulsa, Oklahoma, Society of Exploration Geophysicists Investigations in Geophysics 3, p. 641–712.

Wannamaker, P.E., 1983, Resistivity structure of the northern Basin and Range: Geothermal Resources Council Special Report 13, p. 345–361.

Wernicke, B., 1992, Cenozoic extensional tectonics of the U.S. Cordillera, *in* Burchfiel, B.C., Lipman, P.W., and Zoback, M.L., eds., The Cordilleran orogen: Conterminous U.S.: Geological Society of America, The Geology of North America, v. G-3, p. 553–581.

Wooden, J.L., Kistler, R.W., and Tosdal, R.M., 1998, Pb isotopic mapping of crustal structure in the northern Great Basin and relationships to Au deposit trends, *in* Tosdal, R.M., ed., Contributions to the gold metallogeny of northern Nevada: U.S. Geological Survey Open-File Report 98-338, p. 20–34.

——1999, Strontium, lead, and oxygen isotopic data for granitoid and volcanic rocks from the northern Great Basin and Sierra Nevada, California, Nevada, and Utah: U.S. Geological Survey Open-File Report 99-569, 20 p.

Zietz, I., Andreasen, G.E., and Cain, J.C., 1970, Magnetic anomalies from satellite magnetometer, Journal of Geophysical Research, v. 75, p. 4007–4015.

Zoback, M.L., McKee, E.H., Blakely, R.J., and Thompson, G.A., 1994, The Northern Nevada rift: Regional tectono-magmatic relations and Miocene stress direction: Geological Society of America Bulletin, v. 106, p. 371–382.